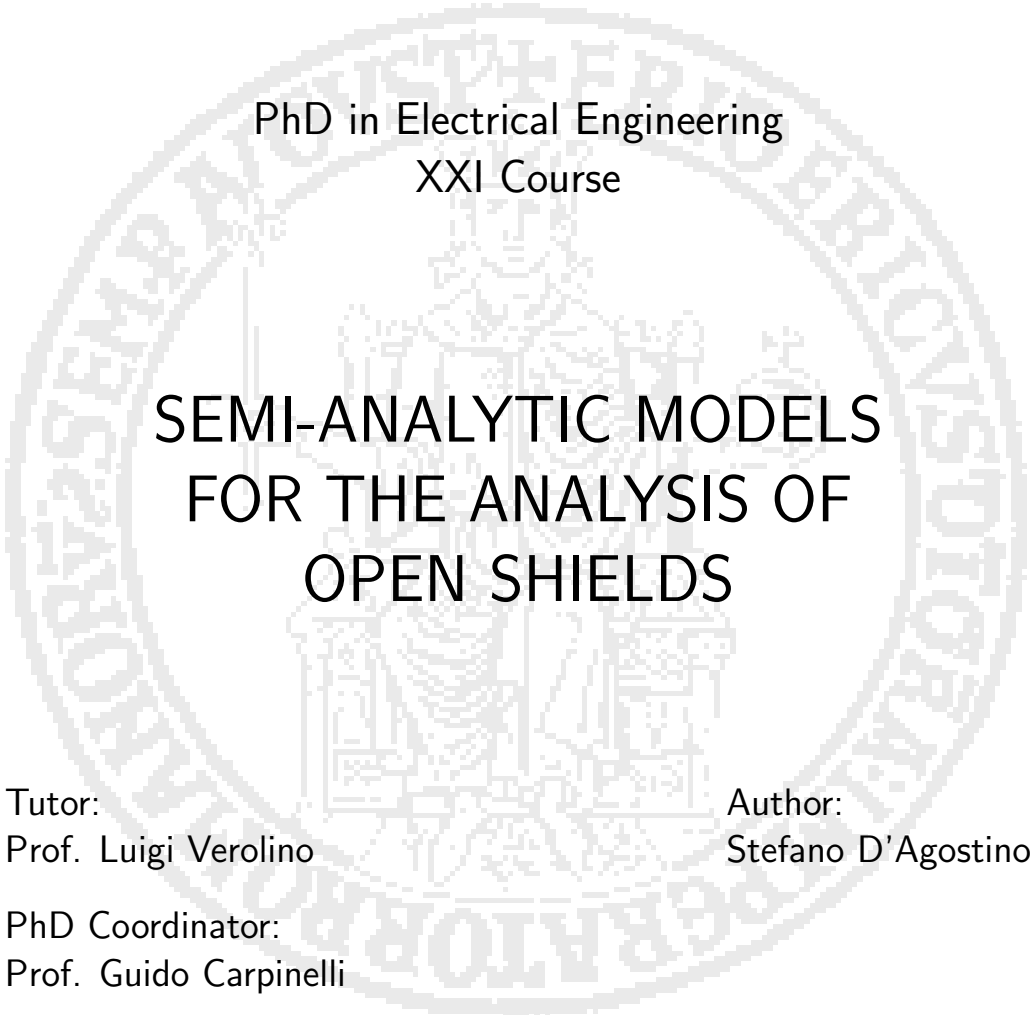


Univeristy "Federico II" of Naples  
Phd School in Industrial Engineering

---

PhD in Electrical Engineering  
XXI Course



SEMI-ANALYTIC MODELS  
FOR THE ANALYSIS OF  
OPEN SHIELDS

Tutor:  
Prof. Luigi Verolino

Author:  
Stefano D'Agostino

PhD Coordinator:  
Prof. Guido Carpinelli

---

December 2008



...to my parents



# Contents

<b>Contents</b>	<b>v</b>
<b>Acknowledgements</b>	<b>vii</b>
<b>1 Introduction</b>	<b>1</b>
1.1 Electromagnetic shielding overview . . . . .	1
1.2 State of the art . . . . .	3
1.3 Summary . . . . .	4
<b>2 Magnetostatic analysis of a thin strip</b>	<b>7</b>
2.1 Problem formulation . . . . .	7
2.2 Induced current . . . . .	9
2.3 Shielding effect . . . . .	13
2.4 Conformal mapping solution . . . . .	15
<b>3 Electromagnetic analysis of thin open structures</b>	<b>19</b>
3.1 Thin Strip . . . . .	19
3.1.1 Induced current . . . . .	19
3.1.2 Shielding effect . . . . .	24
3.2 Coupled thin strips . . . . .	26
3.2.1 Induced current . . . . .	27
3.2.2 Shielding effect . . . . .	30
3.3 Strip array . . . . .	33
3.4 Thin Wedge . . . . .	37

<b>4</b>	<b>Electromagnetic analysis of a thick strip</b>	<b>45</b>
4.1	Induced current . . . . .	45
4.2	Shielding effect . . . . .	48
<b>5</b>	<b>An improved procedure for the convergence acceleration</b>	<b>53</b>
	<b>Conclusions</b>	<b>57</b>
<b>A</b>	<b>Line current source</b>	<b>59</b>
	<b>Bibliography</b>	<b>63</b>

# Acknowledgements

First of all, I have to thank my tutor, prof. Luigi Verolino, for everything he taught me during my academic path. I want to express my gratitude to Dario Assante for his friendly and fundamental support, despite of time and distances.

I cannot forget the prof. Guido Carpinelli for his outstanding courtesy, having always encouraged me to carry on this work.

I must thank Paul Bates and my team at TAC UK for providing me with the time and the serenity to complete this PhD ... I won't forget it.



# Chapter 1

## Introduction

Electromagnetic shielding is the process of limiting the flow of electromagnetic fields between two locations, in order to prevent coupling of undesired electromagnetic energy into devices or systems otherwise susceptible to it.

Interest in this subject dates back more than 50 years, involving critical design aspects in several disciplines (e.g. Electrical machines, Power distribution, Electronics, RF, Measurement systems, etc.).

More recently, there has been an increased interest in the subject because of the growing concern about possible health effects and diseases induced by electromagnetic fields.

### 1.1 Electromagnetic shielding overview

In the 1930's and 1940's, Levy and Schelkunoff wrote on shielding the magnetic fields of a circular current loop by a thin plane metal sheet of infinite extent [1], [2]. Interest in this and related problems grew and spawned special issues of the IEEE Transaction On Electromagnetic Compatibility on the subject of electromagnetic shielding in 1968 and 1988. The aim of this work was the protection of sensitive electronic devices from external electromagnetic fields and the prevention of the leakage of signals from a device which might cause interference.

Several aspects have to be considered for the analysis of the shielding process.

The first is shielding topology.

*Closed* topologies are defined as shield geometries which completely divide space into "source" and "shielded" regions. Examples are infinite planar shields, cylindrical shields and spherical shields. It is worth noting that for these closed topologies the entire current circuit must be inside the source region. Thus, a single line current source rounded by a cylindrical shield would violate the assumptions because its return current would be at infinity, outside of the source region.

*Open* topologies are defined as shield geometries which do not completely separate the source and shielded regions. In this case, the electromagnetic fields may *leak* through seams, holes or around the edges of the shield as well as penetrate through it [3].

A second aspect of shielding is type of material. Shielding materials have usually been characterized as magnetic and/or conducting. The former is a high permeability material and is used to shield by a mechanism called *flux shunting*. In this case, the magnetic flux from a source is diverted into the magnetic material and away from the region to be shielded. The latter is a high conductivity material and is used to shield by a mechanism known as *eddy current cancellation*. In this case, currents are induced in the conductor which cause electromagnetic fields that partially cancel those of the source. These two shielding methods are characterized by different boundary conditions [4]. In the flux shunting case, the tangential component of the magnetic field is nearly zero while in the eddy current cancellation case, the normal component of the magnetic field is nearly zero. It is also useful to note that the effectiveness of closed shields is dependent upon the type of material and the size of the shield. Specifically, it has been found that the eddy current shield mechanism works better for larger diameter closed shields of a given thickness while the flux shunting mechanism works better for smaller diameter closed shields of a given thickness [5]. For open planar shields, which are object of this thesis, it has been shown that the relative effectiveness of flux shunting and eddy current shields depends upon the location of the field point and the size of the shield [4].

A third aspect of shielding is source type, location, and orientation [6]. The

effectiveness of finite width shields has been shown to depend upon the height of the source above the shield [4]. It is also expected that the magnetic fields of sources near the edges of a shield will be shielded differently from the ones located further from the edges. Source orientation with respect to edges is another issue. This can be illustrated as follows. Consider the magnetic field of a source in the absence of a shield. If a perfect flux shunting shield with a zero tangential magnetic field boundary condition is placed along a surface for which the source tangential magnetic field is already zero, then the shield has no effect on the field. If, however, the source is rotated so that the tangential magnetic field along the shield is no longer zero, then the shield will disturb the field and shielding may occur. Thus, source orientation is an important factor to consider.

## 1.2 State of the art

As mentioned in the above section, the first problem about the shielding to be solved was a thin infinite planar shield separating a loop current from the shielded region [1, 2, 6, 7, 8, 9, 10]. The goal of that work was to calculate the penetration of fields through a homogeneous shield characterized by otherwise arbitrary scalar electrical constants. A number of improvements to this original work have been made over the years such as the consideration of multiple layers [11] and replacement of the homogeneous layer by an infinite screen [12]. Similar work has been carried out for shields with cylindrical and spherical geometries [13, 14, 15]. In that work, the sources are cylindrical or spherical dipoles (or multipoles) respectively and the goal is to calculate the penetration of fields through imperfect shielding materials.

In the above works, authors have proposed several solutions, design charts, experimental results; most of them are based on transmission line model [2, 11, 18] for field penetration through the shield. In some cases, closed form expressions have been achieved for closed shields, being their geometry coincident with entire constant coordinate contours in a separable coordinate system.

Nowadays numerical methods are used to analyze and design electromagnetic shields [4, 16, 17, 19] including those comparable to the moment method and,

in particular, the finite element method (FEM).

Although numerical methods allow to achieve solutions for complicated geometries and are relatively simple to be implemented in their up-to-date commercial distributions, such as solutions exhibit a number of limitation in terms of accuracy, range of applicability and numerical computation. In addition, numerical methods are often time consuming and can obscure the fundamental physics of the problem and, hence, may not easily lead to a proper understanding of the electromagnetic phenomenon and do not help to identify the best shield for a given application.

### 1.3 Summary

This thesis deals with the analysis of the shielding effect of open and planar metallic (PEC) structures. Such as structures can realize suitable shields in many different scenarios, from the ELF (Extra Low frequency) to RF and high frequency radiation. The induced current on the PEC structure is responsible for the shielding effect, namely such as current sustains an electromagnetic field which is partially opposed to the source one, causing a field attenuation in some regions.

In this work, an analytic approach will be followed for both the magnetostatic problem (representing a good approximation for ELF shielding) and the electromagnetic one. All the results will be compared with FEM simulations and, where possible, with other solution known in literature.

- In chapter 2 a magnetostatic analysis of a finite width thin PEC strip will be introduced. The problem of the evaluation of the induced current on a thin strip in presence of a stationary line current will be formulated in terms of a Cauchy's type integral equation. The magnetic shielding factor will be evaluated and some sample plots shown.
- In chapter 3 a full-wave electromagnetic analysis of several thin PEC structure will be introduced, such as strips, coupled and arrays of strips and thin wedges. This solution could provide an useful tool for the simulation of several shielding scenarios.

- 
- In chapter 4 the analysis will be extended to thick PEC strip.
  - In chapter 5 an improved procedure to accelerate the electromagnetic analysis convergence will be discussed, in order to reduce the computational time and to achieve better accuracy.



# Chapter 2

## Magnetostatic analysis of a thin strip

In this chapter a magnetostatic analysis of a thin PEC strip fed by a stationary current line is introduced. The problem of the evaluation of the induced current is formulated in terms of a Cauchy's type integral equation which, by means of an adequate polynomial expansion of the kernel, leads to an analytic closed form solution. The analytic expression for the magnetic field in the whole plane and the shielding efficiency are calculated. These results are validated by means of comparison with numerical FEM analysis obtained using Maxwell 2D, a commercial software for EM simulations by Ansoft.

### 2.1 Problem formulation

Let us consider the structure depicted in Figure 2.1: a stationary current line source, namely  $i(t) = I$ , parallel to the  $z$ -axis is located at  $(a, b)$ , in presence of a perfectly conducting infinitesimal strip. The strip is thin, indefinite along the  $z$ -axis, has width  $2D$ , and is placed at  $y = 0$ . It is well known that the magnetic field sustained by a stationary current line in the free space is

$$\mathbf{H}_0(x, y) = \frac{I}{2\pi} \frac{(b - y)\hat{\mathbf{x}} + (x - a)\hat{\mathbf{y}}}{(x - a)^2 + (y - b)^2}. \quad (2.1.1)$$

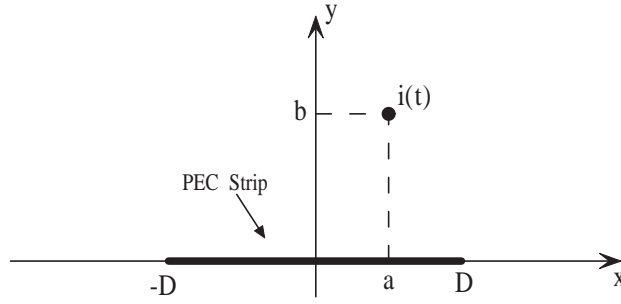


Figure 2.1: Geometry of a thin PEC strip fed by a current line

Because of the particular forcing field and strip geometry, an unknown current density  $\mathbf{J}_0(x) = J_0(x)\hat{\mathbf{z}}$  is induced on the strip, acting along the  $z$ -axis and depending only on  $x$ ; therefore, the field sustained by the induced current is given by the integral representation

$$\mathbf{H}(x, y) = \frac{1}{2\pi} \int_{-D}^D \frac{-y\hat{\mathbf{x}} + (x - x_0)\hat{\mathbf{y}}}{(x - x_0)^2 + y^2} J_0(x_0) dx_0. \quad (2.1.2)$$

Being the strip perfectly conducting, the normal component of the total magnetic field must vanish on it, namely

$$H_y(x, 0) + H_{0y}(x, 0) = 0, \quad |x| \leq D. \quad (2.1.3)$$

Consequently, in order to determine the unknown induced current density, the following integral equation has to be solved

$$\int_{-D}^D \frac{J_0(x_0)}{x - x_0} dx_0 = -I \frac{x - a}{(x - a)^2 + b^2}, \quad |x| \leq D. \quad (2.1.4)$$

A factorization procedure of this Cauchy's integral equation that reduces it to an Abel type integral equation and provide a solution method, is accurately discussed by Estrada and Kanwal [20].

However, in the next section an alternative method of solution, based on a representation of the unknown in an adequate series of orthogonal polynomial functions is presented. The reason why this method has been developed will be clear afterwards, when the obtained magnetostatic solution will be used as

an effective tool to accelerate the dynamic solution convergence.

## 2.2 Induced current

Let us expand the unknown  $J_0$  of the (2.1.4) according to the series

$$J_0(x_0) = \frac{1}{\pi} \frac{I}{\sqrt{D^2 - x_0^2}} \sum_{n=0}^{\infty} S_n T_n(x_0/D), \quad (2.2.1)$$

where  $S_n$  are unknown coefficients, and  $T_n(\cdot)$  are Tchebychev polynomials of the first kind and order  $n$ . This expansion exhibits several interesting features; in particular, it is useful to factorize the right ends behaviour, prescribed by Meixner's condition [23] and necessary to the uniqueness of the solution. Thus, the integral equation (2.1.4) becomes

$$\frac{1}{\pi} \sum_{n=0}^{\infty} S_n \int_{-D}^D \frac{1}{x - x_0} \frac{T_n(x_0/D)}{\sqrt{D^2 - x_0^2}} dx_0 = -\frac{x - a}{(x - a)^2 + b^2}, \quad |x| \leq D. \quad (2.2.2)$$

The kernel

$$K(x, x_0) = \frac{1}{x - x_0} \quad (2.2.3)$$

can be conveniently expanded as follows [20, 24]

$$\frac{1}{x - x_0} = -\frac{2}{D} \sum_{m=1}^{+\infty} T_m(x_0/D) U_{m-1}(x/D), \quad (2.2.4)$$

where  $U_m(\cdot)$  are Tchebychev polynomials of the second kind and order  $m$ .

The last expansion enables the unknown and the kernel to be represented according to the same expansion base and, in force of the orthogonality of the Tchebychev polynomials of first kind,

$$\int_{-1}^1 \frac{T_n(x) T_m(x)}{\sqrt{1 - x^2}} dx = \begin{cases} 0, & m \neq n \\ \frac{\pi}{2}, & m = n \neq 0 \\ \pi, & m = n = 0 \end{cases} \quad (2.2.5)$$

leads to the integrals representation

$$-\frac{D}{\pi} \int_{-D}^D \frac{1}{x-x_0} \frac{T_n(x_0/D)}{\sqrt{D^2-x_0^2}} dx_0 = \begin{cases} 0, & n=0, \\ U_{n-1}(x/D), & n=1, 2, 3, \dots \end{cases} \quad (2.2.6)$$

The value of these integrals for  $n=0$  does not allow the evaluation the first current expansion coefficient  $S_0$ , which has to be imposed by means of physical considerations. Therefore, the integral problem can be rewritten as

$$\frac{1}{D} \sum_{n=1}^{+\infty} S_n U_{n-1}(x/D) = I \frac{x-a}{(x-a)^2 + b^2}. \quad (2.2.7)$$

In force of the orthogonality of Tchebychev polynomials of the second kind,

$$\int_{-1}^1 \sqrt{1-x^2} U_n(x) U_m(x) dx = \begin{cases} 0, & m \neq n \\ \frac{\pi}{2}, & m = n \end{cases} \quad (2.2.8)$$

it follows that

$$S_m = \frac{I}{\pi^2 D} \int_{-D}^D \sqrt{D^2-x_0^2} U_{m-1}(x_0/D) \frac{x-a}{(x-a)^2 + b^2} dx. \quad (2.2.9)$$

Thus, the integral equation (2.1.4) has been inverted, and the induced current density (2.2.1) is

$$\begin{aligned} \pi \sqrt{D^2-x_0^2} J_0(x_0) &= S_0 + \\ &+ \frac{I}{\pi^2 D} \sum_{n=1}^{\infty} T_n(x_0/D) \int_{-D}^D \sqrt{D^2-x_0^2} U_{n-1}(x_0/D) \frac{x-a}{(x-a)^2 + b^2} dx. \end{aligned} \quad (2.2.10)$$

By inverting the order of summation and integration, and using again the expansion (2.2.4), the induced density current can be written as

$$J_0(x_0) = \frac{1}{\pi \sqrt{D^2-x_0^2}} \left[ S_0 - \frac{I}{\pi} \int_{-D}^D \frac{\sqrt{D^2-x^2}}{x-x_0} \frac{(x-a)}{(x-a)^2 + b^2} dx \right] \quad (2.2.11)$$

This is the integral representation of the induced current density, according with the one found by Estrada and Kanwal [20], even if obtained in a completely different way.

It is worth noting that this solution is given with an indeterminate constant, which is going to be evaluated by imposing that the whole current  $I$  uses the strip as return conductor:

$$\int_{-D}^D J(x_0) dx_0 = -I \Rightarrow S_0 = -I. \quad (2.2.12)$$

The solution valid under this assumption is

$$\pi\sqrt{D^2 - x_0^2}J_0(x_0) = -I - \frac{I}{\pi} \int_{-D}^D \frac{\sqrt{D^2 - x^2}}{x - x_0} \frac{(x - a)}{(x - a)^2 + b^2} dx \quad (2.2.13)$$

Performing the integral, a closed form representation of the induced currents is

$$J_0(x) = \frac{I}{\pi\sqrt{D^2 - x^2}} \frac{aC(a, b)(x - a) - b^2/C(a, b)}{(x - a)^2 + b^2}, \quad (2.2.14)$$

where for sake of shortness the function

$$C(x, y) = \frac{1}{|x|\sqrt{2}} \sqrt{\sqrt{(x^2 - y^2 - D^2)^2 + 4x^2y^2} + x^2 - y^2 - D^2} \quad (2.2.15)$$

has been introduced that will be used in the representation of the magnetic field too.

In Figure 2.2 the behavior of the induced current is plotted and compared with the one obtained by Maxwell 2D, a FEM method analysis software by Ansoft.

Most of the applications induce to consider a two line differential supply instead of a single line one. Thus, by means of superposition, the effect of a two line supply is presented in Figure 2.3. Let us, now, present some remarkable cases. If the current line is centered with respect to the strip, namely  $a = 0$ , it follows

$$C(0, b) = \frac{|b|}{\sqrt{b^2 + D^2}} \Rightarrow J_0(x) = -\frac{I}{\pi\sqrt{D^2 - x^2}} \frac{|b|\sqrt{b^2 + D^2}}{x^2 + b^2}. \quad (2.2.16)$$

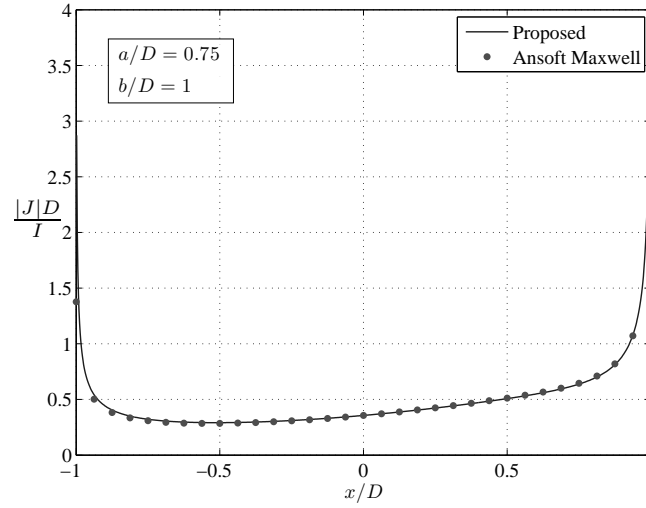


Figure 2.2: Induced current on a thin strip fed by a stationary current line

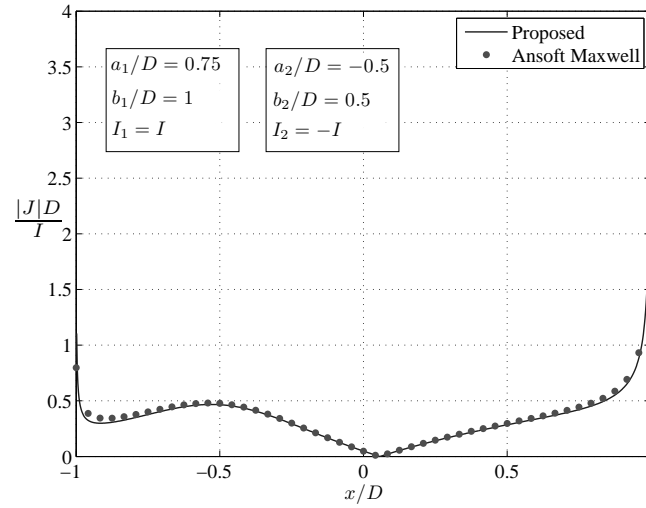


Figure 2.3: Induced current on a thin strip fed by two stationary current line

On the contrary, if the current line lies on the strip plane, namely  $b = 0$  and  $a > D$ , it is

$$C(a, 0) = \frac{1}{|a|\sqrt{2}} \sqrt{|a^2 - D^2| + a^2 - D^2} \Rightarrow J_0(x) = \frac{I}{\pi\sqrt{D^2 - x^2}} \frac{aC(a, 0)}{x - a}. \quad (2.2.17)$$

If the strip is very large, namely  $D \rightarrow \infty$ ,

$$C(a, b) \rightarrow 0 \Rightarrow J_0(x) = -\frac{I|b|}{\pi} \frac{1}{(x-a)^2 + b^2}, \quad (2.2.18)$$

which is the well known result achievable by means of the images theorem.

## 2.3 Shielding effect

The field sustained by the induced current can be then evaluated by the integral (2.1.2). Introducing the following functions

$$R(x, y) = -\frac{a^3C - 2b^2x - 2a^2C^2x + a[C^2(x^2 + y^2) - b^2(C^2 - 2)]}{C\{[b^2 + (a-x)^2]^2 + 2(a-b-x)(a+b-x)y^2 + y^4\}}, \quad (2.3.1)$$

$$U(x, y) = \frac{b^2[(a-x)(a(2C^2 - 1) + x) + b^2 - y^2]}{C\{[b^2 + (a-x)^2]^2 + 2(a-b-x)(a+b-x)y^2 + y^4\}}, \quad (2.3.2)$$

where  $C = C(a, b)$ .

The magnetic field (2.1.2) can be written as

$$H_x(x, y) = \frac{I}{2\pi} y \left\{ \frac{R(x, y)[xC(x, y) + (x-a)/C(x, y)] - U(x, y)/C(x, y)}{\sqrt{(x^2 - y^2 - D^2)^2 + 4x^2y^2}} + \frac{aC(a, b)R(x, y) + U(x, y)/C(a, b)}{\sqrt{(a^2 - b^2 - D^2)^2 + 4a^2b^2}} \right\} \quad (2.3.3)$$

$$H_y(x, y) = \frac{I}{2\pi} \left\{ \frac{R(x, y)[xC(x, y) + (x-a)/C(x, y)] - U(x, y)/C(x, y)}{\sqrt{(x^2 - y^2 - D^2)^2 + 4x^2y^2}} + \frac{aC(a, b)S(x, y) + [U(x, y)(x-a) + b^2T(x, y)]/C(a, b)}{\sqrt{(a^2 - b^2 - D^2)^2 + 4a^2b^2}} \right\} \quad (2.3.4)$$

A contour plot of the magnetic field sustained by the induced current is shown in Figure 2.4.

The expressions (2.3.3), (2.3.4) and (2.1.1) allow the evaluation of the mag-

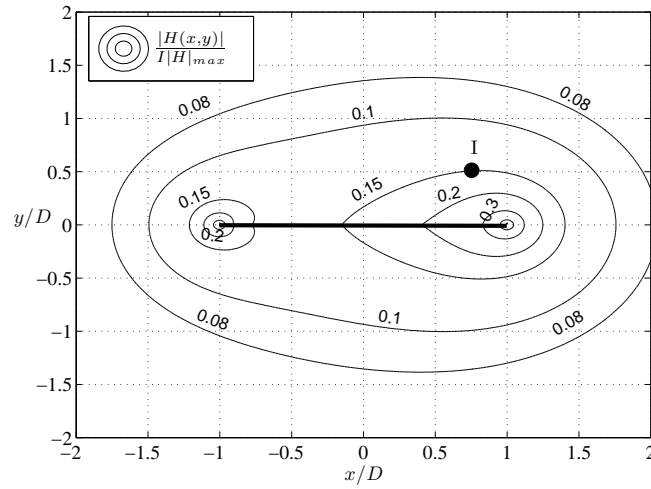


Figure 2.4: Scattered magnetic field of a thin strip fed by a stationary current line

netic shielding factor

$$SE_H(x, y) = 20 \log_{10} \left| \frac{\mathbf{H}(x, y) + \mathbf{H}_0(x, y)}{\mathbf{H}_0(x, y)} \right|. \quad (2.3.5)$$

In Figure 2.5 the contour level of the shielding factor for a thin strip fed by a dual current supply is shown. It is worth noting that in some regions a positive shielding factor is exhibited, due to the effect of the diverging currents at the strip edges.

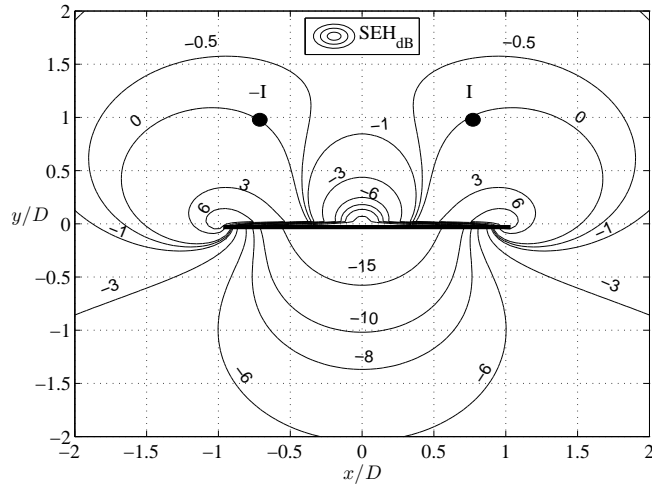


Figure 2.5: Shielding factor of a thin PEC strip fed by two stationary current lines

## 2.4 Conformal mapping solution

In this section we compare the proposed solution of the magnetostatic problem with the result obtained by means of a conformal mapping method. In [22, 25, 26], the magnetostatic problem has been analytically solved introducing the following transformation to the complex domain:

$$z = D \frac{1 - \tau^2}{1 + \tau^2}, \quad (2.4.1)$$

being  $z = x + jy$  the field point and  $\tau = u + jv$  the corresponding point in the mapped plane. This transformation reduce magnetic field evaluation to the problem of a current line over an infinite perfectly conductive plane which can be easily solved by means of the images theorem.

Thus, the magnetic field can be found as

$$H_x = -\Im m \left\{ \frac{dw}{dz} \right\}, \quad (2.4.2)$$

$$H_y = -\Re e \left\{ \frac{dw}{dz} \right\}, \quad (2.4.3)$$

where,

$$\frac{dw}{dz} = \frac{I}{2\pi} \left( \frac{1}{\tau - \tau_0} - \frac{1}{\tau - \tau_0^*} - \frac{1}{\tau - j} + \frac{1}{\tau + j} \right) \frac{d\tau}{dz}, \quad (2.4.4)$$

$$\frac{d\tau}{dz} = -\frac{(1 + \tau^2)^2}{4D\tau}, \quad (2.4.5)$$

$$\tau = \pm \sqrt{\frac{D - z}{D + z}}, \quad (2.4.6)$$

and  $\tau_0^*$  is the complex conjugate of  $\tau_0$ . In (2.4.6) the minus sign has to be used when  $y > 0$ , the plus sign otherwise.

It is very interesting to highlight that in the (2.4.4), the first two terms of the sum represent, respectively, the current line source and its image; then two other sources have been introduced at  $\pm j$  to represent the current return lines at the infinity. It is now apparent that a completely different approach has been introduced in the above sections, assuming that the return conductor for the current is the strip itself.

In the applications a real return conductor is always present (the current source must be a proper circuit), therefore in most of the results presented in literature the superposition of the dual current line, namely  $I$  and  $-I$ , does hide this choice.

In Figure 2.6 the proposed solution is compared with the conformal mapping one and the FEM analysis. It is clear that the solution achieved in this work does agree with the FEM simulation in any case (both single line supply and dual one), the conformal mapping one exhibits a completely different behaviour in case of single current line (in which case the total induced current on the strip is zero, being the current returned at infinity). In Figure 2.7 comparison between the proposed method and the conformal mapping solution, for a dual current line is shown.

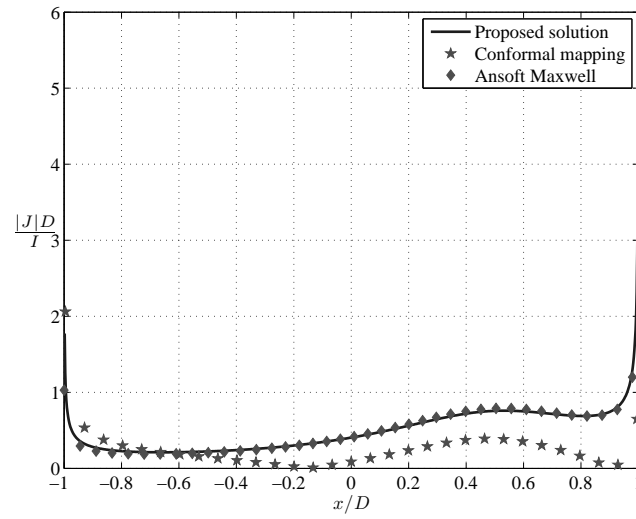


Figure 2.6: Induced current on a thin strip fed by a single current line - Comparison with conformal mapping solution

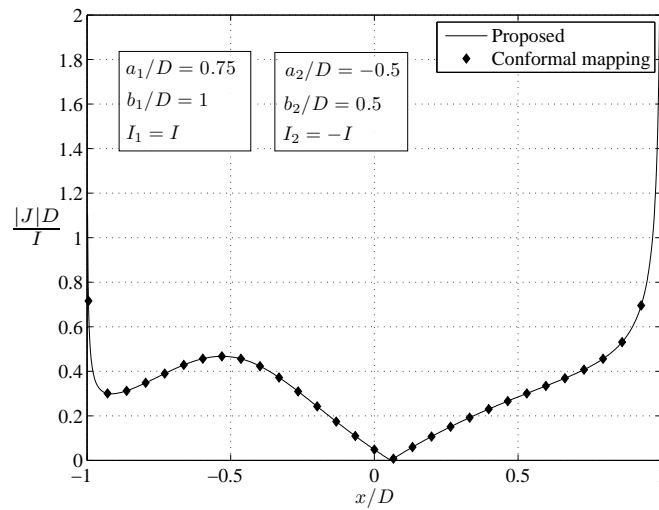


Figure 2.7: Induced current on a thin strip fed by a dual current line - Comparison with conformal mapping solution



# Chapter 3

## Electromagnetic analysis of thin open structures

In this chapter the electromagnetic analysis of several PEC open shields is introduced. The induced current on thin shields, array of thin shields, and thin wedges are calculated by means of a semi-analytic approach. The electric and magnetic shielding effect of these structure are evaluated.

### 3.1 Thin Strip

#### 3.1.1 Induced current

The geometry of the problem is depicted in figure 3.1. A dynamic current line

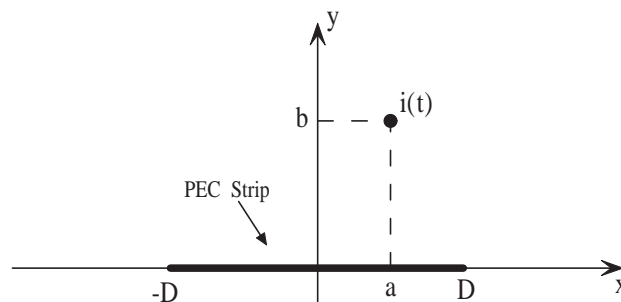


Figure 3.1: Geometry of a thin PEC strip fed by a current line

source, namely  $I = I(\omega)$ , parallel to the  $z$ -axis is located at  $(a, b)$ , in presence of a perfectly conducting infinitesimal strip. The strip is thin, indefinite along the  $z$ -axis, has width  $2D$ , and is placed at  $y = 0$ . It is well known that the electromagnetic field sustained by a dynamic current line in the free space is

$$\mathbf{E}_0(x, y) = -\hat{\mathbf{z}}\zeta_0 \frac{k}{4} I(\omega) H_0^{(2)} \left[ k \sqrt{(x-a)^2 + (y-b)^2} \right], \quad (3.1.1)$$

$$\mathbf{H}_0(x, y) = j \frac{k}{4} I(\omega) H_1^{(2)} \left[ k \sqrt{(x-a)^2 + (y-b)^2} \right] \frac{(y-b)\hat{\mathbf{x}} - (x-a)\hat{\mathbf{y}}}{\sqrt{(x-a)^2 + (y-b)^2}}, \quad (3.1.2)$$

where  $\zeta_0 = \sqrt{\mu_0/\varepsilon_0}$  is the characteristic impedance of the free space,  $k = \omega\sqrt{\varepsilon_0\mu_0}$  is the wavenumber,  $I(\omega)$  is impressed source current in the frequency Fourier domain, and  $H_\nu^{(2)}(\cdot)$  is the Hankel function of the second kind and order  $\nu$ . As in the stationary case, the unknown current density  $\mathbf{J}(x) = J(x)\hat{\mathbf{z}}$  on the strip sustains an electromagnetic field, which can be written as

$$\mathbf{E}(x, y) = -\hat{\mathbf{z}}\zeta_0 \frac{k}{4} \int_{-D}^D J(x_0) H_0^{(2)} \left[ k \sqrt{(x-x_0)^2 + y^2} \right] dx_0, \quad (3.1.3)$$

$$\mathbf{H}(x, y) = j \frac{k}{4} \int_{-D}^D J(x_0) H_1^{(2)} \left[ k \sqrt{(x-x_0)^2 + y^2} \right] \frac{y\hat{\mathbf{x}} - (x-x_0)\hat{\mathbf{y}}}{\sqrt{(x-x_0)^2 + y^2}} dx_0. \quad (3.1.4)$$

The boundary condition imposes that the tangential component of the total electric field must vanish on the strip, namely

$$E_z(x, 0) + E_{0z}(x, 0) = 0, \quad |x| \leq D. \quad (3.1.5)$$

Therefore, the induced current has to verify the following integral equation

$$\int_{-D}^D J(x_0) H_0^{(2)} [k|x-x_0|] dx_0 = -I(\omega) H_0^{(2)} \left[ k \sqrt{(x-a)^2 + b^2} \right], \quad |x| \leq D. \quad (3.1.6)$$

In order to solve this problem, let us expand the unknown similarly to magnetostatic case, according to series (2.2.1)

$$J(x_0) = \frac{1}{\pi} \frac{I(\omega)}{\sqrt{D^2 - x_0^2}} \sum_{n=0}^{\infty} F_n T_n(x_0/D). \quad (3.1.7)$$

Since Meixner's condition [23] for the dynamic analysis is the same of the magnetostatic one, the expansion (3.1.7) does correctly factorizes the behaviour at the edges, and the integral equation (3.1.6) becomes

$$\frac{1}{\pi} \sum_{n=0}^{\infty} F_n \int_{-D}^D H_0^{(2)}[k|x - x_0|] \frac{T_n(x_0/D)}{\sqrt{D^2 - x_0^2}} dx_0 = -H_0^{(2)} \left[ k \sqrt{(x - a)^2 + b^2} \right],$$

$$|x| \leq D. \quad (3.1.8)$$

It is worth noting that the kernel of this integral equation

$$K(x, x_0) = H_0^{(2)}[k|x - x_0|] \quad (3.1.9)$$

cannot be expanded in terms of Tchebychev polynomials, as already done in stationary case. However, the integral equation (3.1.6) can be reduced to a system of linear equations by multiplying for

$$\frac{T_m(x/D)}{\sqrt{D^2 - x^2}}, \quad m = 0, 1, 2, \dots, \quad (3.1.10)$$

and integrating from  $-D$  to  $D$  with respect to  $x$ . Thus, by truncating the serie to an adequate coefficient  $N$ , the linear system is

$$\begin{pmatrix} A_{00} & \dots & A_{0N} \\ \vdots & \ddots & \vdots \\ A_{N0} & \dots & A_{NN} \end{pmatrix} \cdot \begin{pmatrix} F_0 \\ \vdots \\ F_N \end{pmatrix} = \begin{pmatrix} b_0 \\ \vdots \\ b_N \end{pmatrix}, \quad (3.1.11)$$

where,

$$A_{nm} = \frac{1}{\pi} \int_{-D}^D \frac{T_m(x/D)}{\sqrt{D^2 - x^2}} \int_{-D}^D \frac{T_n(x_0/D)}{\sqrt{D^2 - x_0^2}} H_0^{(2)} [k|x - x_0|] dx_0 dx, \quad (3.1.12)$$

$$b_m = - \int_{-D}^D \frac{T_m(x/D)}{\sqrt{D^2 - x^2}} H_0^{(2)} \left[ k\sqrt{(x - a)^2 + b^2} \right] dx. \quad (3.1.13)$$

The matrix element  $A_{nm}$  is, in effect, a double integral, but in force of the integral representation of the Hankel function of the second kind [31]

$$H_0^{(2)} [k|x - x_0|] = \frac{1}{\pi} \int_{-\infty}^{+\infty} \frac{\cos[w(x - x_0)]}{\sqrt{k^2 - w^2}} dw, \quad (3.1.14)$$

it can be reduced to a single improper integral. By substituting (3.1.9) into (3.1.12), the expression of the  $A_{nm}$  becomes

$$A_{nm} = \frac{1}{\pi^2} \int_{-D}^D \frac{T_m(x/D)}{\sqrt{D^2 - x^2}} \int_{-D}^D \frac{T_n(x_0/D)}{\sqrt{D^2 - x_0^2}} \int_{-\infty}^{+\infty} \frac{\cos[w(x - x_0)]}{\sqrt{k^2 - w^2}} dw dx_0 dx. \quad (3.1.15)$$

Now, by interchanging the order of integration and by using the relevant integrals [31]

$$\int_{-D}^D \frac{T_n(x/D)}{\sqrt{D^2 - x^2}} \cos(wx) dx = \begin{cases} 0, & \text{if } n \text{ is odd,} \\ (-1)^{\frac{n}{2}} \pi J_n(wD), & \text{if } n \text{ is even,} \end{cases} \quad (3.1.16)$$

$$\int_{-D}^D \frac{T_n(x/D)}{\sqrt{D^2 - x^2}} \sin(wx) dx = \begin{cases} (-1)^{\frac{n-1}{2}} \pi J_n(wD), & \text{if } n \text{ is odd,} \\ 0, & \text{if } n \text{ is even,} \end{cases} \quad (3.1.17)$$

can be, finally, obtained

$$A_{nm} = (-j)^{n+m} \int_{-\infty}^{+\infty} \frac{J_n(wD) J_m(wD)}{\sqrt{k^2 - w^2}} dw, \quad (3.1.18)$$

where  $J_\mu(\cdot)$  is a Bessel functions of first kind and order  $\mu$ . It is worth noting that the linear system equation here obtained is the same given in [21] but it has been achieved without introducing any spatial fourier transforms following an even more simple and effective path. All the integrals (3.1.18) and (3.1.13) can

be numerically evaluated. An adequate transformation on the complex plane [21] allows to evaluate the  $A_{nm}$  integrals over a finite range of integration, namely

$$A_{nm} = 2(-j)^{n+m} \int_0^{\pi/2} J_n(kD \sin \tau) H_m^{(2)}(kD \sin \tau) d\tau, \quad n \geq m, \quad (3.1.19)$$

providing a remarkable computational benefit.

In Figure 3.2 and 3.3 are, respectively, plotted the behaviour of the induced current and the expansion coefficients for different position of the source line. It is worth noting that the closer the current source is ( $b \rightarrow 0$ ), the slower is the series convergence. This highlights that this method does suffer the proximity effect, therefore in Chapter 5 an improved procedure to accelerate the series convergence will be introduced.

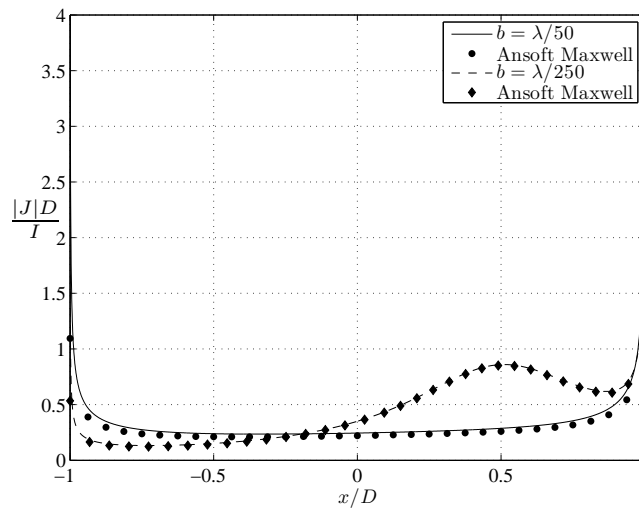


Figure 3.2: Induced current for different values of  $b$  ( $a = \lambda/200$  and  $D = \lambda/100$ ).

Figure 3.4 shows the induced current on a thin strip fed by a dual current source displaced at  $(a_1, b)$  and  $(a_2, b)$ .

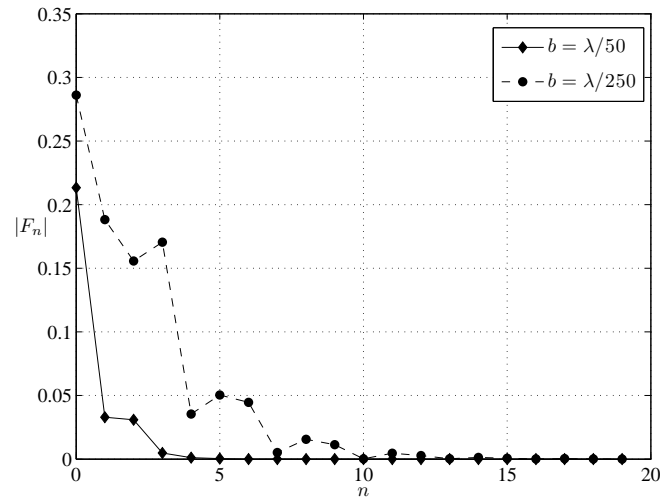


Figure 3.3: Magnitude of the expansion coefficients for different values of  $b$  ( $a = \lambda/200$  and  $D = \lambda/100$ ).

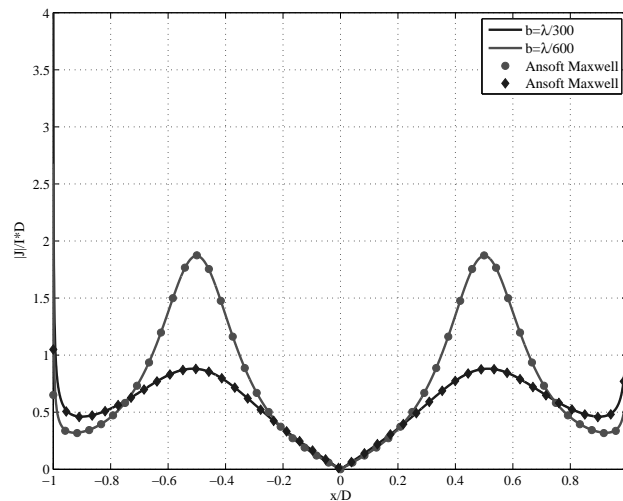


Figure 3.4: Induced current for different values of  $b$  (dual current source supply -  $|a_{1,2}| = \lambda/200$  and  $D = \lambda/100$ ).

### 3.1.2 Shielding effect

The numerical evaluation of the total electromagnetic field in the whole  $(x, y)$ -plane, by integrating the (3.1.3) and (3.1.4), allows the representation of the

shielding effect of the thin PEC strip. Let us remember the definition of the shielding factor [25, 28]

$$SE_H(x, y) = 20 \log_{10} \left| \frac{\mathbf{H}(x, y) + \mathbf{H}_0(x, y)}{\mathbf{H}_0(x, y)} \right|, \quad (3.1.20)$$

for the magnetic field, and

$$SE_E(x, y) = 20 \log_{10} \left| \frac{\mathbf{E}(x, y) + \mathbf{E}_0(x, y)}{\mathbf{E}_0(x, y)} \right|, \quad (3.1.21)$$

for the electric field.

The shielding factor for the magnetic and electric fields, in presence of a two differential dynamic line source, is, respectively, depicted in Figure 3.5 and 3.6.

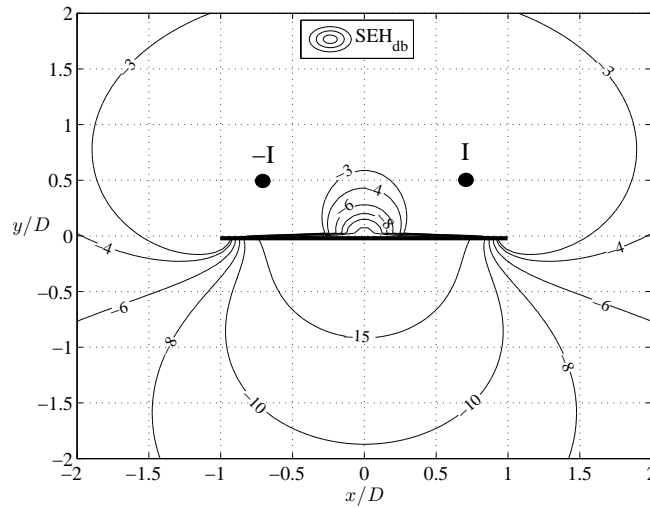


Figure 3.5: Magnetic field shielding factor -  $D = \lambda/150$

In Figure 3.7 the shielding factor for both the magnetic and the electrical fields is shown against the frequency. This graphics can be very useful to determinate the frequency range of application for a shield.

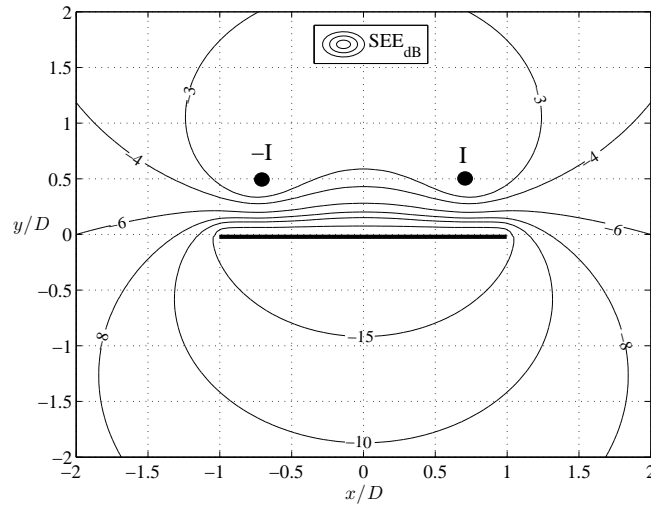


Figure 3.6: Electric field shielding factor -  $D = \lambda/150$

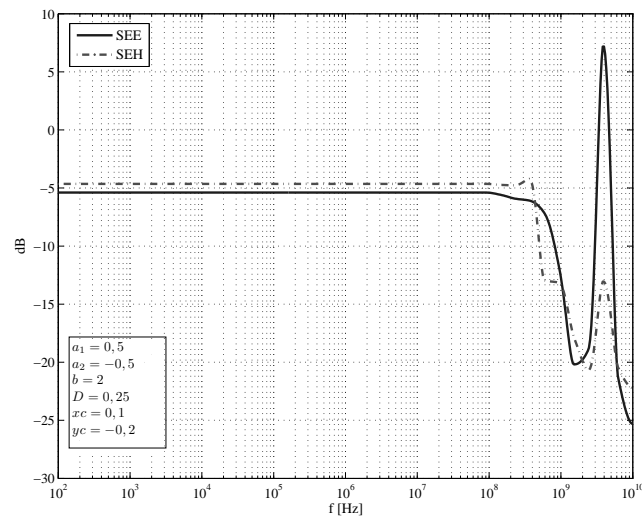


Figure 3.7: Shielding factor at the test point  $(x_c, y_c)$  against the current frequency.

## 3.2 Coupled thin strips

In this section the electromagnetic analysis of coupled thin PEC strip arrays is introduced. The problem of the evaluation of the induced current is formulated

in terms of a system of integral equations and solved by means of the collocation method. Different shielding structures can be accurately simulated using this solution method (shields with aperture, shielding grids, wire shielding meshes, etc.). All the results are validated by means of comparison with FEM analysis and the shielding factor is plotted for some sample geometries.

### 3.2.1 Induced current

The problem geometry, two PEC strips fed by a dynamic current line  $I(\omega)$  placed at  $(a, b)$ , is depicted in Figure 3.8. The strips are centered at  $\pm C$  and

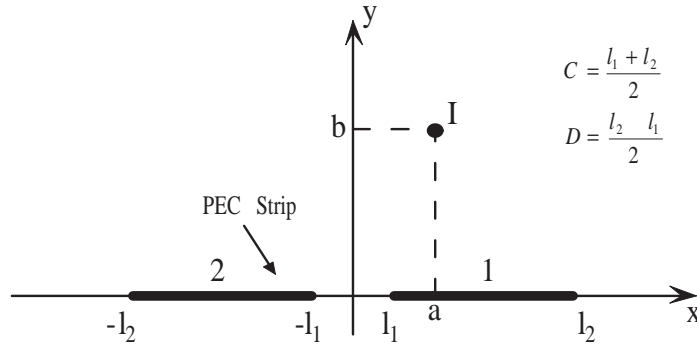


Figure 3.8: Two coupled thin strips fed by a current line source

have width  $2D$ . As the electric field sustained by the induced current can be written as

$$E_{1z}(x, y) = -\zeta_0 \frac{k}{4} \int_{l_1}^{l_2} J_1(x_0) H_0^{(2)} \left[ k \sqrt{(x - x_0)^2 + y^2} \right] dx_0, \quad (3.2.1)$$

$$E_{2z}(x, y) = -\zeta_0 \frac{k}{4} \int_{-l_2}^{-l_1} J_2(x_0) H_0^{(2)} \left[ k \sqrt{(x - x_0)^2 + y^2} \right] dx_0, \quad (3.2.2)$$

by imposing the tangential electric field condition on both the strips:

$$E_{0z}(x, 0) + E_{1z}(x, 0) + E_{2z}(x, 0) = 0, \quad x \in (-l_2, -l_1) \cup (l_1, l_2) \quad (3.2.3)$$

the evaluation of the induced current is reduced to the following integral problem

$$\int_{l_1}^{l_2} J_1(x_0) H_0^{(2)} [k|x - x_0|] dx_0 + \int_{-l_2}^{-l_1} J_2(x_0) H_0^{(2)} [k|x - x_0|] dx_0 = -I(\omega) H_0^{(2)} \left[ k\sqrt{(x-a)^2 + b^2} \right], \quad x \in (-l_2, -l_1) \cup (l_1, l_2) \quad (3.2.4)$$

assuming, respectively, for the first and the second integral of the right hand  $t = x_0 - C$  and  $t = x_0 + C$ , the problem becomes

$$\int_{-D}^D J_1(t) H_0^{(2)} [k|x - t - C|] dt + \int_{-D}^D J_2(t) H_0^{(2)} [k|x - t + C|] dt = -I(\omega) H_0^{(2)} \left[ k\sqrt{(x-a)^2 + b^2} \right], \quad x \in (-l_2, -l_1) \cup (l_1, l_2) \quad (3.2.5)$$

Expanding the induced currents according with

$$J_i(t) = \frac{I}{\sqrt{1 - (t/D)^2}} \sum_{n=0}^{\infty} F_{i,n} T_n(t/D), \quad i = 1, 2 \quad (3.2.6)$$

it leads to the following system:

$$\begin{aligned} & \sum_{n=0}^{\infty} F_{1,n} \int_{-D}^D \frac{T_n(t/D)}{\sqrt{1 - (t/D)^2}} H_0^{(2)} [k|x - t - C|] dt + \\ & \sum_{n=0}^{\infty} F_{2,n} \int_{-D}^D \frac{T_n(t/D)}{\sqrt{1 - (t/D)^2}} H_0^{(2)} [k|x - t + C|] dt = \\ & -I(\omega) H_0^{(2)} \left[ k\sqrt{(x-a)^2 + b^2} \right], \quad x \in (-l_2, -l_1) \cup (l_1, l_2) \end{aligned} \quad (3.2.7)$$

A simple and effective method of solution for such a kind of equations system is the "collocation". By truncating the two series to  $N$  terms and sampling both members of the equation in  $N$  points (on the strip itself), a system of algebraic equations is obtained, whose solution gives the current expansion coefficients. Besides, to minimize the representation error, it can be shown [27] that the best choice for the sampling points is the zeros of Tchebychev polynomials of

the first kind, namely

$$T_{N+1}(x_k/D) = 0 \rightarrow x_k = D \cos \left( \frac{2k+1}{N+1} \frac{\pi}{2} \right), \quad k = 0, 1, \dots, N.$$

Moreover, this choice makes the coefficients value more stable with respect to the truncation order of the series.

Thus, provided the collocation points as the zeros of  $T_{N+1}(x/D)$ ,  $x_{1,0}, \dots, x_{1,N} \in (l_1, l_2)$  and  $x_{2,0}, \dots, x_{2,N} \in (-l_2, -l_1)$ , the problem can be reduced to the solution of an equivalent system of linear equations:

$$\begin{pmatrix} a_{00} & \dots & a_{0N} & b_{00} & \dots & b_{0N} \\ \vdots & \ddots & \vdots & \vdots & \ddots & \vdots \\ a_{N0} & \dots & a_{NN} & b_{N0} & \dots & b_{NN} \\ c_{00} & \dots & c_{0N} & d_{00} & \dots & d_{0N} \\ \vdots & \ddots & \vdots & \vdots & \ddots & \vdots \\ c_{N0} & \dots & c_{NN} & d_{N0} & \dots & d_{NN} \end{pmatrix} \cdot \begin{pmatrix} F_{1,0} \\ \vdots \\ F_{1,N} \\ F_{2,0} \\ \vdots \\ F_{2,N} \end{pmatrix} = \begin{pmatrix} p_0 \\ \vdots \\ p_N \\ q_0 \\ \vdots \\ q_N \end{pmatrix}, \quad (3.2.8)$$

where

$$a_{m,n} = \int_{-D}^D W_n(t, D) H_0^{(2)}(k|x_{1,m} - t - C|) dt, \quad (3.2.9)$$

$$b_{m,n} = \int_{-D}^D W_n(t, D) H_0^{(2)}(k|x_{1,m} - t + C|) dt, \quad (3.2.10)$$

$$c_{m,n} = \int_{-D}^D W_n(t, D) H_0^{(2)}(k|x_{2,m} - t - C|) dt, \quad (3.2.11)$$

$$d_{m,n} = \int_{-D}^D W_n(t, D) H_0^{(2)}(k|x_{2,m} - t + C|) dt, \quad (3.2.12)$$

$$p_k = -H_0^{(2)} \left( k \sqrt{(x_{1,m} - a)^2 + b^2} \right), \quad (3.2.13)$$

$$q_k = -H_0^{(2)} \left( k \sqrt{(x_{2,m} - a)^2 + b^2} \right). \quad (3.2.14)$$

$$(3.2.15)$$

and

$$W_n(t, D) = \frac{T_n(t/D)}{\sqrt{1 - (t/D)^2}}. \quad (3.2.16)$$

In order to improve the numerical computation of the matrix elements integrals, because of the diverging behavior at the edges given by  $1/\sqrt{1 - (t/D)^2}$ , it is worth introducing a cosine transform  $t = D \cos \tau$ . Thus,

$$a_{m,n} = L \int_0^\pi \cos(n\tau) H_0^{(2)}(k|x_{1,m} - D \cos \tau - C|) d\tau, \quad (3.2.17)$$

accelerating the integration algorithm convergence and achieving better accuracy.

In Figure 3.9 and 3.10 are plotted the induced current on two coupled strip fed respectively by single and dual line current. The obtained behaviour is compare with a FEM simulations via Ansoft Maxwell 2D.

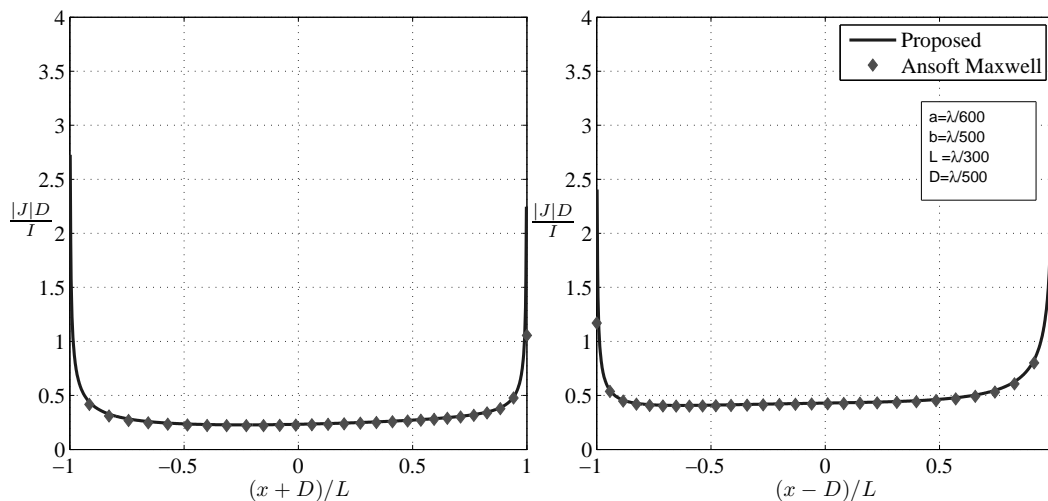


Figure 3.9: Induced current on two coupled thin strips fed by a single current line

### 3.2.2 Shielding effect

Very often aperture are needed in the shields, to allow ventilation, wired connections and others kind of interaction with the external environment, there-

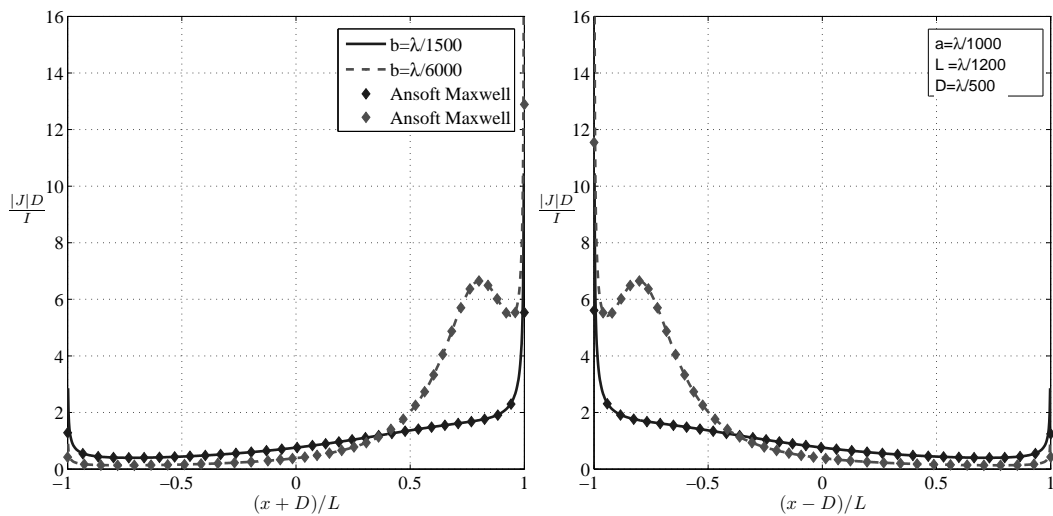


Figure 3.10: Induced current on two coupled thin strips fed by a dual current line for different source position  $b$

fore such as solution provides a very useful simulation and analysis tool. In Figure 3.11 and 3.12 the contour lines for the electric and magnetic shielding factor is plotted.

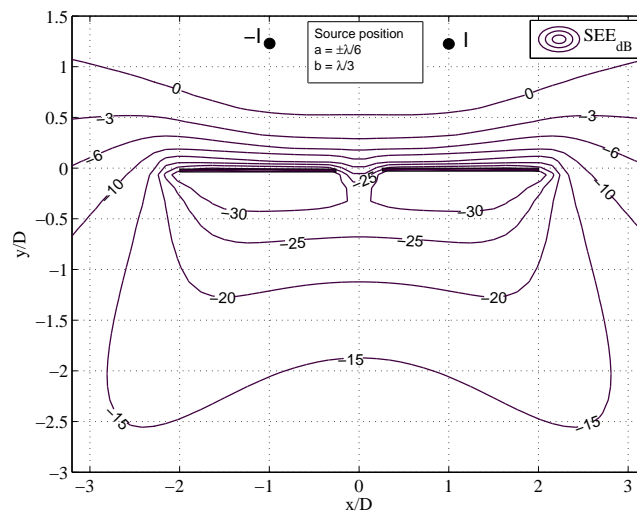


Figure 3.11: Electric shielding factor for two coupled strips. The distance between the strips is  $\lambda/10$

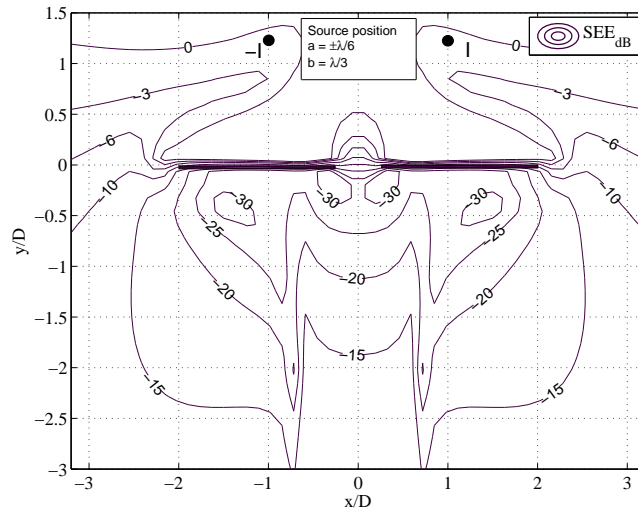


Figure 3.12: Magnetic shielding factor for two coupled strips. The distance between the strips is  $\lambda/10$

It is worth noting how the fields leak inside the shield as the aperture grows in terms of wavelength. In the Figure 3.13 the spectrum of both the electric and magnetic shielding factor is reported for a coupled strips shield (aperture); it is clear that as soon as the impressed current wavelength approaches the dimension of the aperture, the fields start penetrating into the shield.

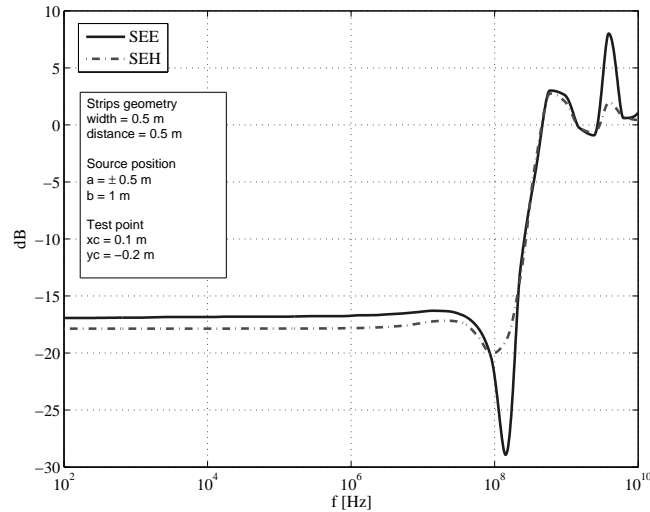


Figure 3.13: Spectrum of the shielding factor for a couple of thin strips

### 3.3 Strip array

The methodology introduced in the above section can be naturally extended to the case of  $N$  planar thin strips, allowing the simulation on several different shields common in the industrial practice (e.g. slotted metallic plates, metallic grids, mesh-wired shields, etc.). In this section a simulation of sample shield constituted by 5 thin strip, as in Figure 3.14 is reported. The magnitude of

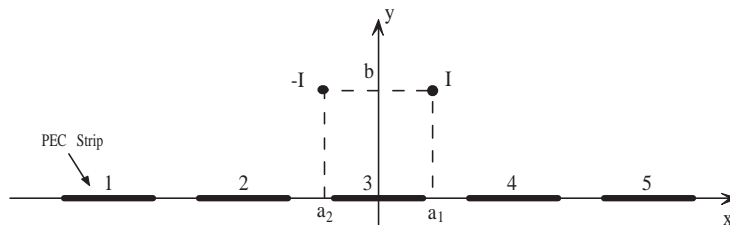


Figure 3.14: Five thin strips array fed by a current line source

the calculated expansion coefficient and the induced current on the five strip is plotted in Figure 3.15. The magnetic and the electric shielding factor have been evaluated and are shown, respectively, in Figure 3.16 and 3.17. The

field leaking through the shield apertures is depending on the frequency of the forcing current, namely the width of the apertures with respect to the wavelength; this is well represented in Figure 3.18, where the shielding factors at the test point  $(x_c, y_c)$  are plotted against the frequency.

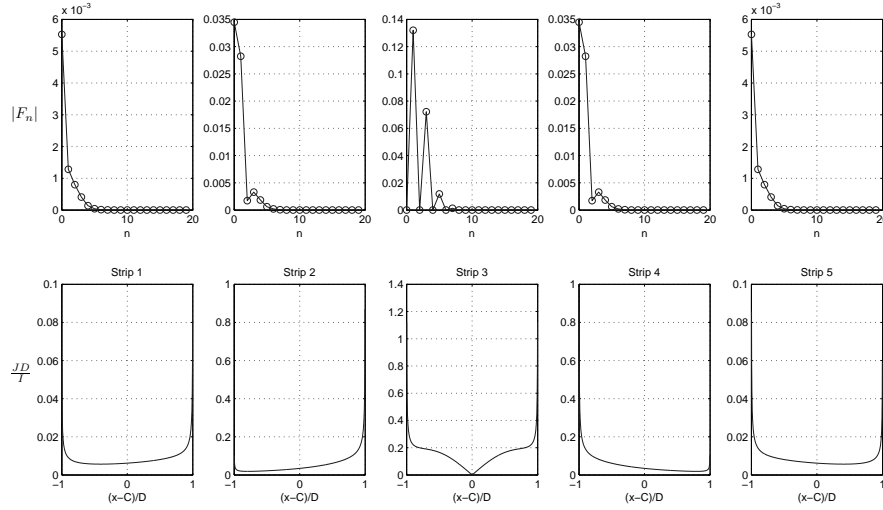


Figure 3.15: Expansion coefficients magnitude and induced current on a 5 PEC strips array.

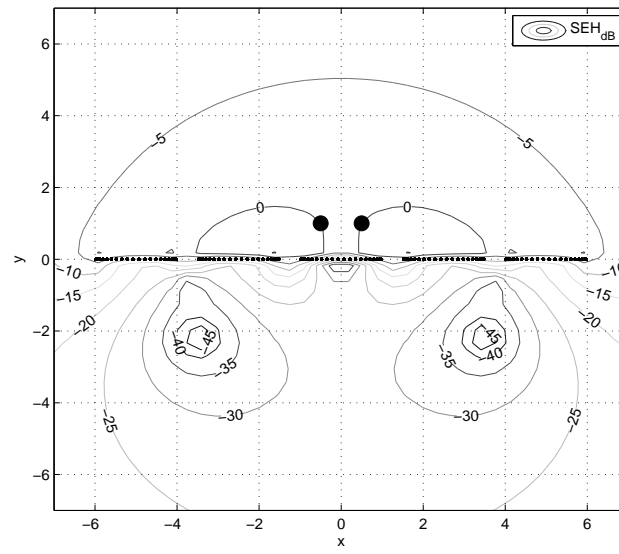


Figure 3.16: Magnetic Shielding Effect of five coupled strips

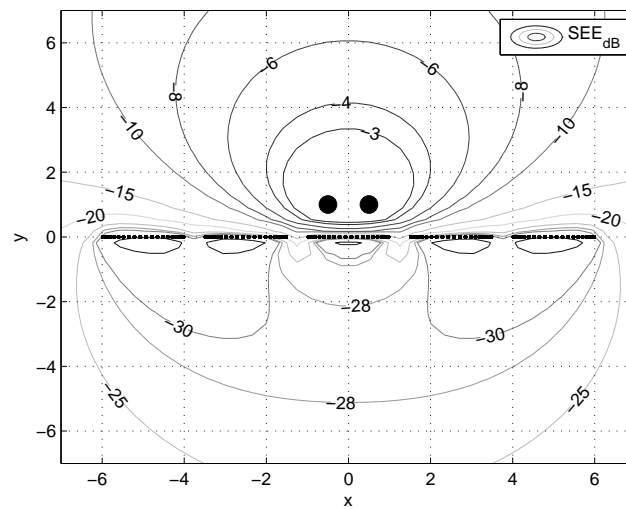


Figure 3.17: Electric Shielding Effect of five coupled strips

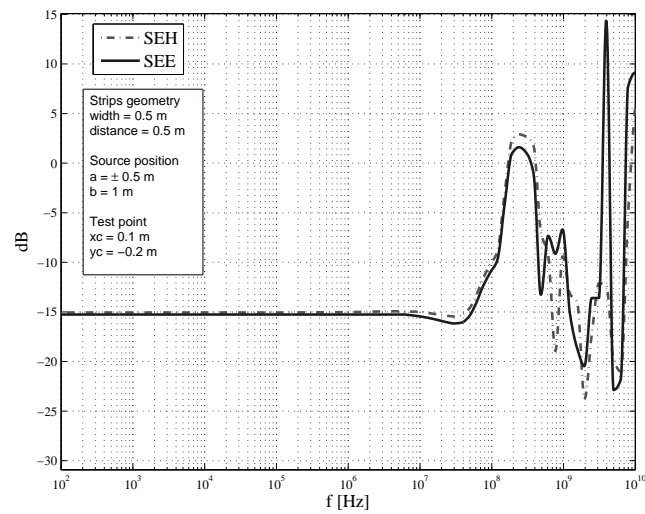


Figure 3.18: Electric Shielding Effect of five coupled strips

### 3.4 Thin Wedge

In this section the induced current on a thin PEC wedge are evaluated and some consideration about the shielding property of these structure are shown.

Provided the structure depicted in Figure 3.19 and 3.20, because of the

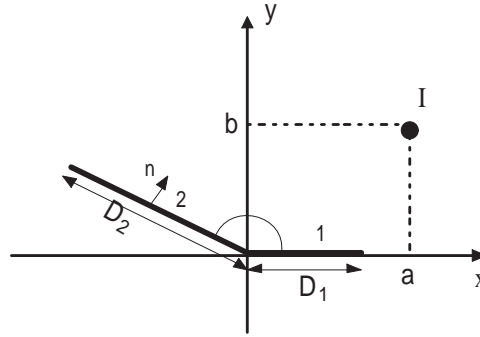


Figure 3.19: Thin "concave" metallic wedge fed by a current line

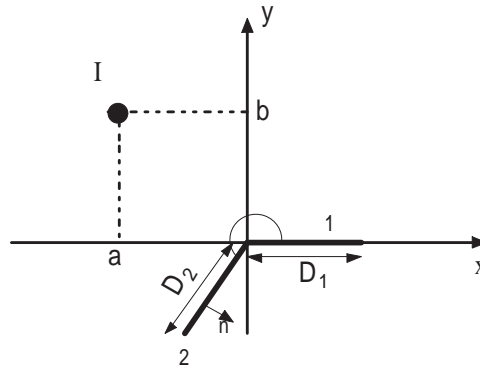


Figure 3.20: Thin "convex" metallic wedge fed by a current line

particular current source, the induce current on the wedge surface will have only the  $z$ -component:  $\mathbf{I} = I\hat{z} \Rightarrow \mathbf{J}(x, y) = J(x, y)\hat{z}$ .

Thus, the electric field sustained by the induced current on the wedge walls 1 and 2 can be respectively written as

$$E_{1z}(x, y) = -\zeta_0 \frac{k}{4} \int_0^{D_1} J_1(t) H_0^{(2)} \left[ k\sqrt{(x-t)^2 + y^2} \right] dt, \quad (3.4.1)$$

$$E_{2z}(x, y) = -\zeta_0 \frac{k}{4} \int_0^{D_2} J_2(t) H_0^{(2)} \left[ k \sqrt{(x - t \cos \alpha)^2 + (y - t \sin \alpha)^2} \right] dt, \quad (3.4.2)$$

provided the following parametric representation on the face 2.

$$\forall t \in (0, D_2) \begin{cases} x = t \cos \alpha \\ y = t \sin \alpha. \end{cases}$$

By imposing the boundary condition on the wedge surface (namely, the total tangential electric field must vanish on it)

$$\begin{cases} E_{0z}(x, 0) + E_{1z}(x, 0) + E_{2z}(x, 0) = 0, & 0 \leq x \leq D_1 \\ E_{0z}(\tau \cos \alpha, \tau \sin \alpha) + E_{1z}(\tau \cos \alpha, \tau \sin \alpha) + E_{2z}(\tau \cos \alpha, \tau \sin \alpha) = 0, \\ & 0 \leq \tau \leq D_2 \end{cases} \quad (3.4.3)$$

the problem can be written in terms of a system of two integral equations.

$$\begin{cases} \int_0^{D_1} J_1(t) H_0^{(2)} [k|x-t|] dt + \int_0^{D_2} J_2(t) H_0^{(2)} [k\sqrt{x^2+t^2-2xt\cos\alpha}] dt \\ = -I(\omega) H_0^{(2)} [k\sqrt{(x-a)^2+b^2}], & x \in (0, D_1) \\ \int_0^{D_1} J_1(t) H_0^{(2)} [k\sqrt{\tau^2+t^2-2\tau t\cos\alpha}] dt + \int_0^{D_2} J_2(t) H_0^{(2)} (k|\tau-t|) dt \\ = -I(\omega) H_0^{(2)} [k\sqrt{\tau^2+a^2+b^2-2\tau(a\cos\alpha+b\sin\alpha)}], & \tau \in (0, D_2) \end{cases} \quad (3.4.4)$$

It is worth noting that if  $\alpha = \pi$  and  $D_1 = D_2 = D$  the problem is reduced to the integral equation of one single thin strip (3.1.6).

The unknown on the wedge surface current can be expanded, according to the solution discussed in the above sections, in a adequate series of Tchebychev orthogonal polynomials, factorizing the edge behavior to satisfy the Meixner condition [23] as

$$J_1(t) = \frac{I(\omega)}{\sqrt{1-(t/D_1)^2}} (t/D_1)^{\frac{\pi}{\alpha}-1} \sum_{n=0}^{\infty} F_n T_n(2t/D_1 - 1), \quad (3.4.5)$$

$$J_2(t) = \frac{I(\omega)}{\sqrt{1 - (t/D_2)}} (t/D_2)^{\frac{\pi}{\alpha} - 1} \sum_{n=0}^{\infty} G_n T_n(2t/D_2 - 1). \quad (3.4.6)$$

Note that for a "convex" wedge,  $\alpha > \pi$  as in figure 3.20, the surface current current is divergent at the vertex; on the contrary, if the wedge is "concave",  $\alpha < \pi$  as in figure 3.19, the current is vanishing at the vertex.

By substituting the expansion (3.4.5) and (3.4.6) in (3.4.4), having introduced the following function

$$W_n(t, L) = \frac{T_n(2t/L - 1)}{\sqrt{1 - (t/L)}} \left(\frac{t}{L}\right)^{\frac{\pi}{\alpha} - 1}, \quad (3.4.7)$$

the problem leads to the following system of integral equations:

$$\left\{ \begin{array}{l} \sum_{n=0}^{\infty} \left( F_n \int_0^{D_1} W_n(t, D_1) H_0^{(2)}[k|x - t|] dt \right. \\ \quad \left. + G_n \int_0^{D_2} W_n(t, D_2) H_0^{(2)}[k\sqrt{x^2 + t^2 - 2xt \cos \alpha}] dt \right) \\ \quad = -H_0^{(2)}[k\sqrt{(x - a)^2 + b^2}], \quad 0 \leq x \leq D_1 \\ \sum_{n=0}^{\infty} \left( F_n \int_0^{D_1} W_n(t, D_1) H_0^{(2)}[k\sqrt{\tau^2 + t^2 - 2\tau t \cos \alpha}] dt \right. \\ \quad \left. + G_n \int_0^{D_2} W_n(t, D_2) H_0^{(2)}[k|\tau - t|] dt \right) \\ \quad = -H_0^{(2)}[k\sqrt{\tau^2 + a^2 + b^2 - 2\tau(a \cos \alpha + b \sin \alpha)}], \quad 0 \leq \tau \leq D_2 \end{array} \right. \quad (3.4.8)$$

Sampling both the equations in  $(x_0, \dots, x_N) \in ]0, D_1[$  e  $(\tau_0, \dots, \tau_N) \in ]0, D_2[$  and truncating both the series to  $N$  order term, the problem is reduced to the solution of a system of linear equations where the unknowns are  $F_0, \dots, F_N$

and  $G_0, \dots, G_N$ .

$$\begin{pmatrix} a_{00} & \dots & a_{0N} & b_{00} & \dots & b_{0N} \\ \vdots & \ddots & \vdots & \vdots & \ddots & \vdots \\ a_{N0} & \dots & a_{NN} & b_{N0} & \dots & b_{NN} \\ c_{00} & \dots & c_{0N} & d_{00} & \dots & d_{0N} \\ \vdots & \ddots & \vdots & \vdots & \ddots & \vdots \\ c_{N0} & \dots & c_{NN} & d_{N0} & \dots & d_{NN} \end{pmatrix} \cdot \begin{pmatrix} F_0 \\ \vdots \\ F_N \\ G_0 \\ \vdots \\ G_N \end{pmatrix} = \begin{pmatrix} p_0 \\ \vdots \\ p_N \\ q_0 \\ \vdots \\ q_N \end{pmatrix}, \quad (3.4.9)$$

where

$$a_{nk} = \int_0^{D_1} W_n(t, D_1) H_0^{(2)}(k|x-t|) dt \quad (3.4.10)$$

$$b_{nk} = \int_0^{D_2} W_n(t, D_2) H_0^{(2)}\left(k\sqrt{x^2+t^2-2xt\cos\alpha}\right) dt \quad (3.4.11)$$

$$c_{nk} = \int_0^{D_1} W_n(t, D_1) H_0^{(2)}\left(k\sqrt{\tau^2+t^2-2\tau t\cos\alpha}\right) dt \quad (3.4.12)$$

$$d_{nk} = \int_0^{D_2} W_n(t, D_2) H_0^{(2)}(k|\tau-t|) dt \quad (3.4.13)$$

$$p_k = -H_0^{(2)}\left(k\sqrt{(x-a)^2+b^2}\right) \quad (3.4.14)$$

$$q_k = -H_0^{(2)}\left(k\sqrt{\tau^2+a^2+b^2-2\tau(a\cos\alpha+b\sin\alpha)}\right) \quad (3.4.15)$$

e  $k = 0, \dots, N$  e  $n = 0, \dots, N$ .

In Figure 3.21 the induced current on a concave PEC wedges are plotted and the proposed solution is compared with a FEM simulation. Then, the electric and magnetic shielding factor are respectively shown in Figure 3.22 and 3.23.

In full analogy with the above sample, Figure 3.24,3.25 and show the current and shielding behaviour for a convex PEC wedge.

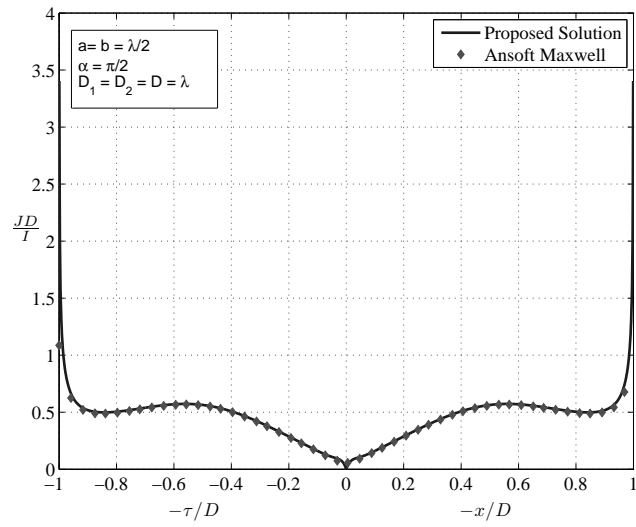


Figure 3.21: Induced current on a "concave" wedge

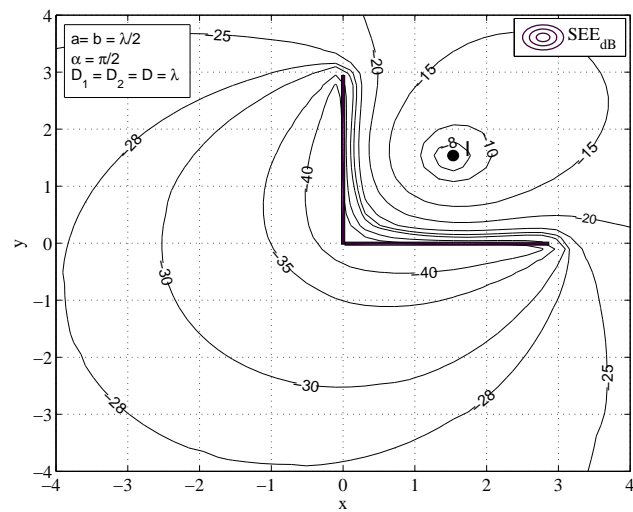


Figure 3.22: Electric shielding factor for a "concave" wedge

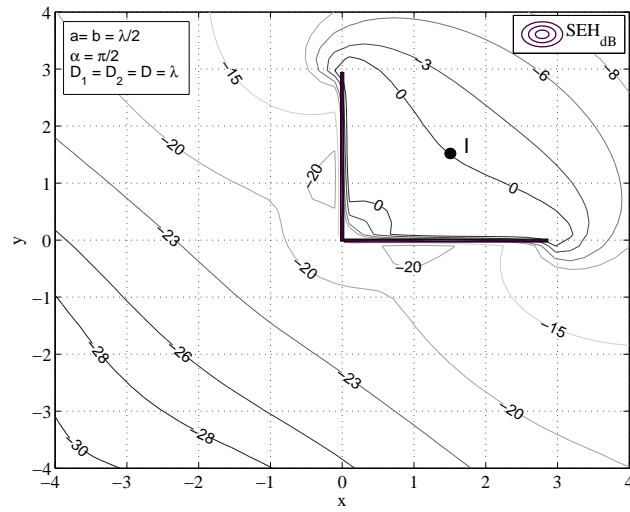


Figure 3.23: Magnetic shielding factor for a "concave" wedge

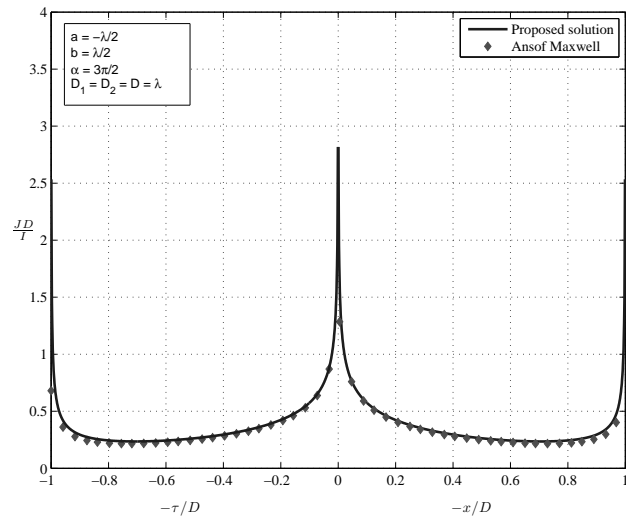


Figure 3.24: Induced current on a "convex" wedge

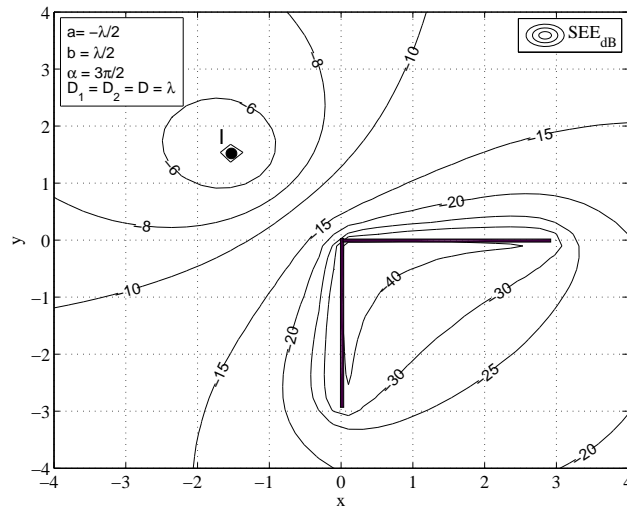


Figure 3.25: Electric shielding factor for a "convex" wedge

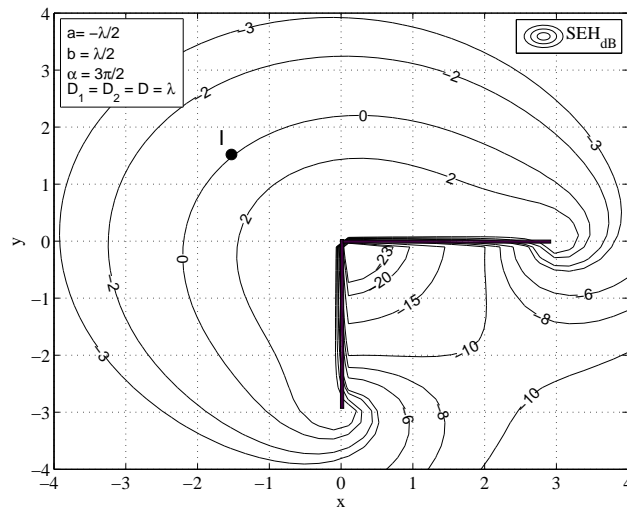


Figure 3.26: Magnetic shielding factor for a "convex" wedge



# Chapter 4

## Electromagnetic analysis of a thick strip

In this chapter is shown how the method introduced in the earlier chapters can be suitably used for the analysis of thick structure (namely, considering the finite thickness of the metallic plates). In order to have an adequate representation of the induced current and solving the integral problem, an expansion in terms of Neumann series has been introduced [29], which is a generalization of the (3.1.7). The solution is validate, again, by means of a comparison with FEM simulations and the shielding factors are computed and plotted.

### 4.1 Induced current

The geometry of the problem is outlined in Figure 4.1, where a PEC strip of width  $2D_x$  and height  $2D_y$ , indefinite along the  $z$ -axis, is centered in the  $(x, y)$  plane in presence of a line current source parallel to the strip  $I = I(\omega)$  at  $(a, b)$ . The same procedure used for the thin strip analysis can be adapted to this problem as long as the induce current on the four strip walls are taken into account. Thus, the electric field sustained by the induced current can be

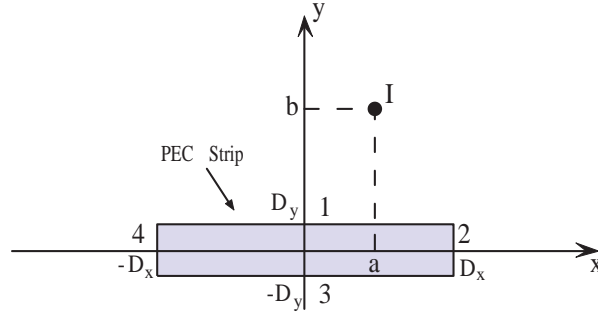


Figure 4.1: Geometry of a thick PEC strip fed by a current line

written as

$$\begin{aligned}
 E_z(x, y) = -\zeta_0 \frac{k}{4} \left\{ \int_{-D_x}^{D_x} J_1(x_0) H_0^{(2)} \left[ k \sqrt{(x - x_0)^2 + (y - D_y)^2} \right] dx_0 + \right. \\
 \int_{-D_y}^{D_y} J_2(y_0) H_0^{(2)} \left[ k \sqrt{(x - D_x)^2 + (y - y_0)^2} \right] dy_0 + \\
 \int_{-D_x}^{D_x} J_3(x_0) H_0^{(2)} \left[ k \sqrt{(x - x_0)^2 + (y + D_y)^2} \right] dx_0 + \\
 \left. \int_{-D_y}^{D_y} J_4(y_0) H_0^{(2)} \left[ k \sqrt{(x + D_x)^2 + (y - y_0)^2} \right] dy_0 \right\}
 \end{aligned} \tag{4.1.1}$$

and the boundary conditions on the four strip walls have to be imposed:

$$\begin{cases} E_{0z}(x, D_y) + E_z(x, D_y) = 0, & |x| \leq D_x \end{cases} \tag{4.1.2}$$

$$\begin{cases} E_{0z}(D_x, y) + E_z(D_x, y) = 0, & |y| \leq D_y \end{cases} \tag{4.1.3}$$

$$\begin{cases} E_{0z}(x, -D_y) + E_z(x, -D_y) = 0, & |x| \leq D_x \end{cases} \tag{4.1.4}$$

$$\begin{cases} E_{0z}(-D_x, y) + E_z(-D_x, y) = 0, & |x| \leq D_x \end{cases} \tag{4.1.5}$$

These conditions lead to a system of integral equations.

In order to solve this system, a suitable expansion of the unknown induced current is needed and, because of the different geometry (in particular, the

different edge angles), the current expansion (3.1.7) used for the thin strip solution does not provide an adequate representation.

For this class of problems solutions by means of the Neumann series [29] have been reported by some authors [21]. The general expansion in terms of Neumann series can be written as

$$J(x) = \frac{I(\omega)}{D_x} \left(1 - \frac{x^2}{D_x^2}\right)^{s-1/2} \sum_{n=0}^{\infty} F_n \frac{2^s n! \Gamma(s)}{j^n \Gamma(2s+n)} C_n^s(x/D_x) \quad (4.1.6)$$

where  $C_n^s(\cdot)$  are the Gegenbauer polynomials of index  $s$  and order  $n$ . The parameter  $s$  has to be chosen to satisfy the behaviour at the edges [23].

It is worth noting that the expansion (3.1.7) is actually the particular case the (4.1.6) for  $s = 0$  [30].

For a thick strip the Meixner condition at the edges imposes  $s = 1/6$ . Thus, the induced current, respectively on the horizontal and vertical walls, can be expanded as

$$J_i(x) = \frac{I(\omega)}{D_x} \frac{1}{\sqrt[3]{1 - (x/D_x)^2}} \sum_{n=0}^{\infty} F_{i,n} C_n^{1/6}(x/D_x), \quad i = 1, 3 \quad (4.1.7)$$

$$J_i(y) = \frac{I(\omega)}{D_y} \frac{1}{\sqrt[3]{1 - (y/D_y)^2}} \sum_{n=0}^{\infty} F_{i,n} C_n^{1/6}(y/D_y), \quad i = 2, 4 \quad (4.1.8)$$

Then, the integral problem becomes

$$\begin{aligned}
& \sum_{n=0}^{\infty} \left\{ F_{1,n} \int_{-D_x}^{D_x} \frac{H_0^{(2)} \left[ k \sqrt{(x-x_0)^2 + (y-D_y)^2} \right]}{D_x \sqrt[3]{1 - (x_0/D_x)^2}} C_n^{1/6}(x_0/D_x) dx_0 + \right. \\
& F_{2,n} \int_{-D_y}^{D_y} \frac{H_0^{(2)} \left[ k \sqrt{(x-D_x)^2 + (y-y_0)^2} \right]}{D_y \sqrt[3]{1 - (y_0/D_y)^2}} C_n^{1/6}(y_0/D_y) dy_0 + \\
& F_{3,n} \int_{-D_x}^{D_x} \frac{H_0^{(2)} \left[ k \sqrt{(x-x_0)^2 + (y+D_y)^2} \right]}{D_x \sqrt[3]{1 - (x_0/D_x)^2}} C_n^{1/6}(x_0/D_x) dx_0 + \\
& \left. F_{4,n} \int_{-D_y}^{D_y} \frac{H_0^{(2)} \left[ k \sqrt{(x+D_x)^2 + (y-y_0)^2} \right]}{D_y \sqrt[3]{1 - (y_0/D_y)^2}} C_n^{1/6}(y_0/D_y) dy_0 \right\} = \\
& = -H_0^{(2)} \left[ k \sqrt{(x-a)^2 + (y-b)^2} \right], \quad \forall (x, y) \text{ on the strip walls}
\end{aligned} \tag{4.1.9}$$

By truncating the series to  $N$  coefficients and sampling the equation (4.1.9) in  $4N$  points on the strip walls, the problem can be reduced to a linear equations system also in this case. Again, in order to improve the method convergence, the sampling point have been chosen as the zeroes of the Tchebychev polynomials of the first kind and order  $N + 1$ .

In Figure 4.2 and 4.3 the induced current on the strip walls are plotted and the proposed analysis is validated by a comparison with a FEM simulation. Figure 4.4 shows the expansion coefficient magnitude of the induced current on the four walls.

## 4.2 Shielding effect

The electric and the magnetic shielding factor is respectively plotted in figure 4.5 and 4.6

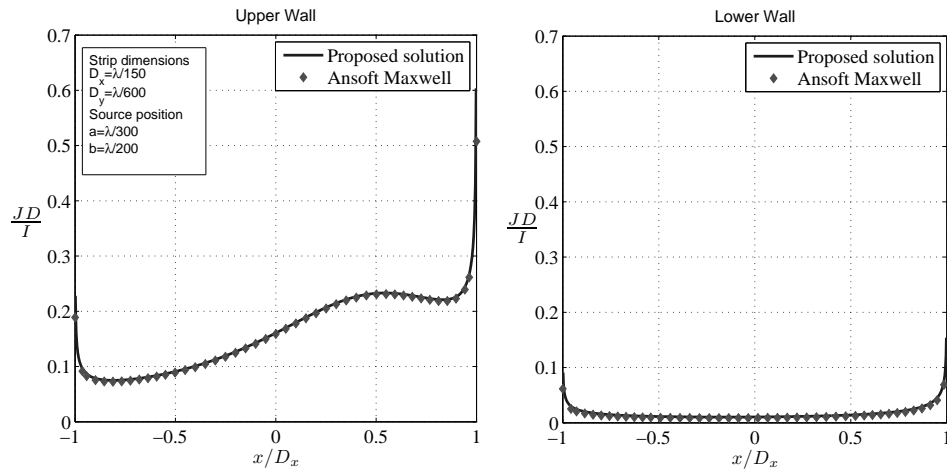


Figure 4.2: Induced current on a thick strip - Upper and lower walls

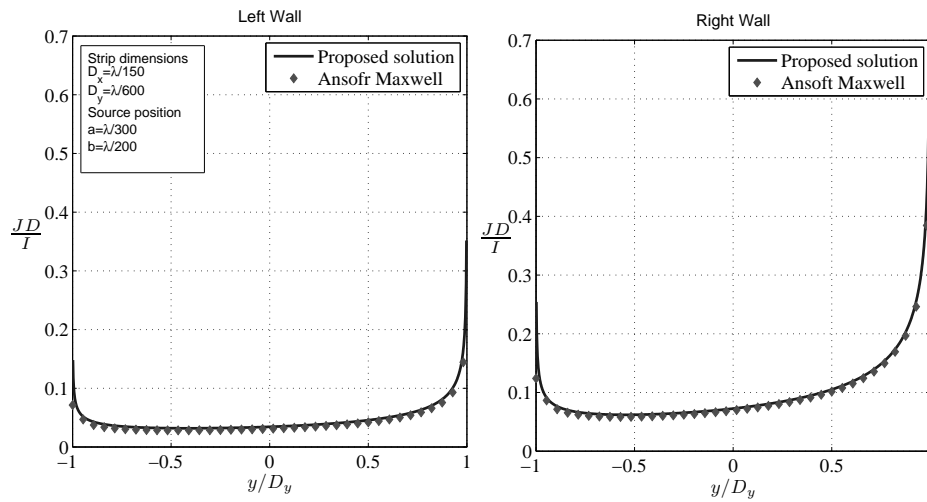


Figure 4.3: Induced current on a thick strip - Upper and lower walls

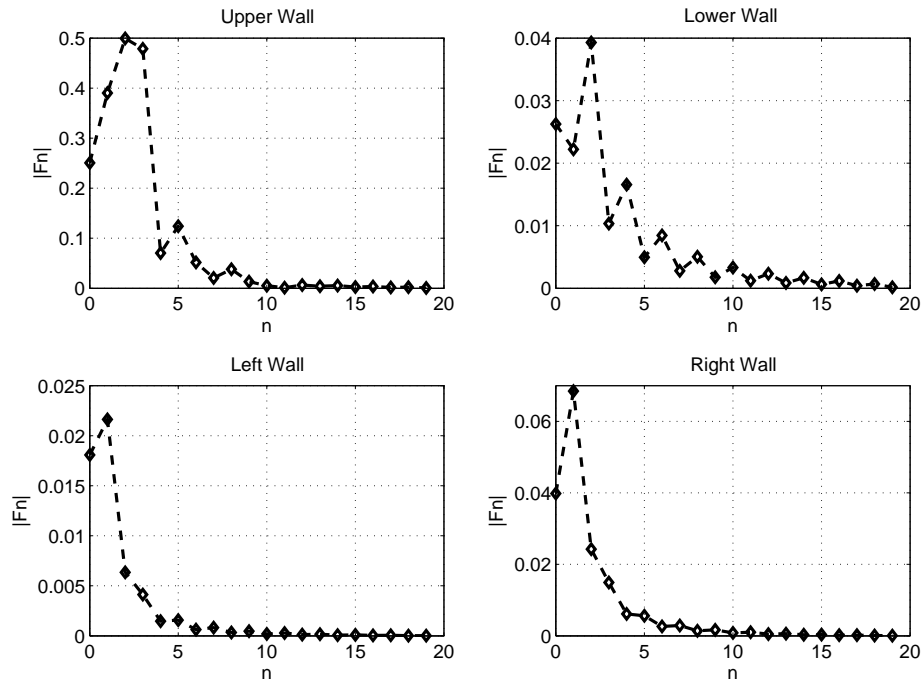


Figure 4.4: Expansion coefficient of the induced current on the four walls of a thick strip

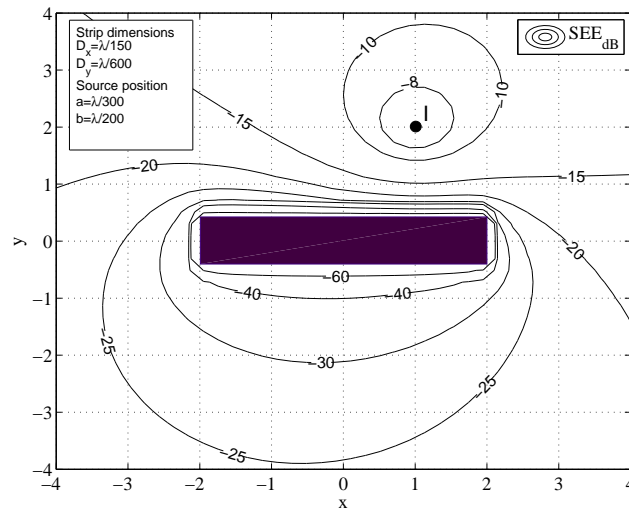


Figure 4.5: Electric shielding factor of a thick strip

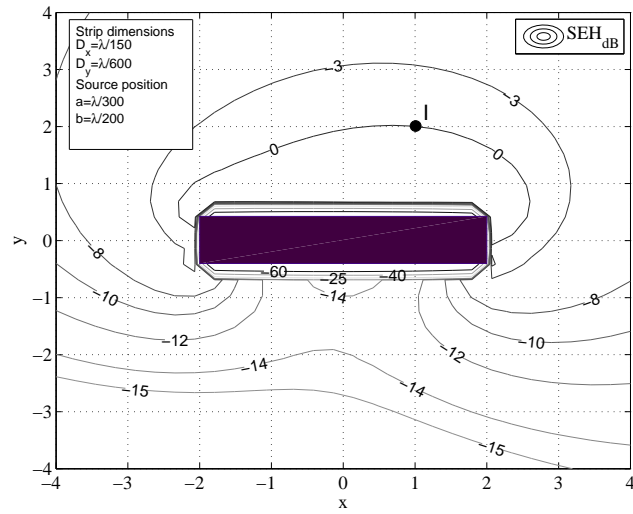


Figure 4.6: Magnetic shielding factor of a thick strip



# Chapter 5

## An improved procedure for the convergence acceleration

In chapter 3 a semi-analytic method for the evaluation of the induced current on a thin PEC strip has been introduced, providing an handful solution in terms of Tchebychev polynomials. In Figure 3.3 has been shown that when current line approaches the strip, a greater number of expansion coefficient is needed. That is because the induced current does present a peak in correspondence of the current line, for  $b \rightarrow 0$  the solution approaches an impulsive function. Thus, it is clear that the proposed method for the electromagnets analysis does "suffer" this proximity effect, becoming slowly convergent and time consuming.

It is interesting to observe that the behavior of the induced current due to a line source very close to the strip it is very similar to the magnetostatic behavior. In force of this observation, the idea, of using the analytic magnetostatic solution to improve the electromagnetic method, has been developed.

The dynamic solution can be written in the variational form

$$\Delta J(x) = J(x) - J_0(x), \quad |x| < D, \quad (5.0.1)$$

where  $J_0(x)$  is the known magnetostatic solution and the incremental expansion coefficients of the new unknown  $\Delta J(x)$  are

$$\Delta F_n = F_n - S_n, \quad (5.0.2)$$

where  $F_n$  and  $S_n$  are respectively the coefficients of the dynamic (3.1.7) and static expansions (2.2.1).

Thus, the new unknown  $\Delta J(x)$  can be evaluated by solving the linear system

$$\underline{\underline{A}} \cdot \underline{\Delta \mathbf{F}} = \mathbf{b} - \underline{\underline{A}} \cdot \mathbf{S}, \quad (5.0.3)$$

where  $\underline{\underline{A}}$  is the  $A_{nm}$  matrix (3.1.18),  $\mathbf{b}$  and  $\underline{\Delta \mathbf{F}}$  are respectively the vector of the  $b_m$  (3.1.13) and  $\Delta F_n$  (5.0.2), and  $\mathbf{S}$  is the vector of  $S_n$  (2.2.9).

In Figure 5.1 the induced currents, obtained by the proposed improved method, are compared with the non accelerated series solution. It is interesting to note that, if  $b = \lambda/1000$ , more than 20 expansion terms are not enough to reconstruct the right behavior, as shown in Figure 5.2, whereas, by means of the proposed incremental method, the currents are accurately reconstructed with only one term.

The introduced procedure does reduce drastically the computational time, allowing this method to be used with good results and accuracy in a very wide range of shielding geometry, frequencies and current sources configurations.

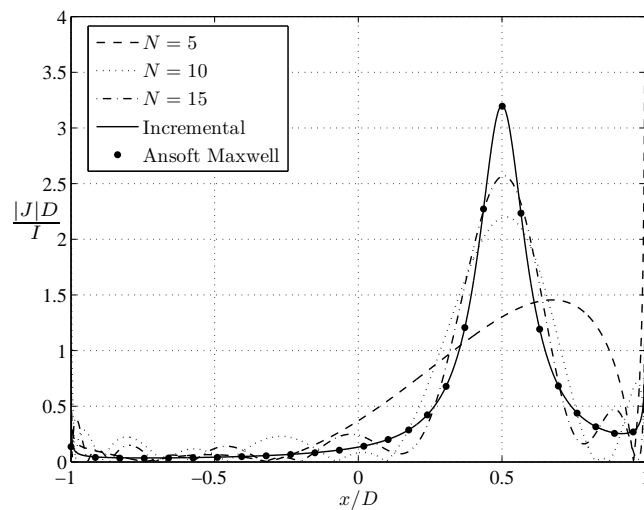


Figure 5.1: Induced current for different values  $N$  of truncation of the series in comparison with the incremental solution and the FEM simulation.

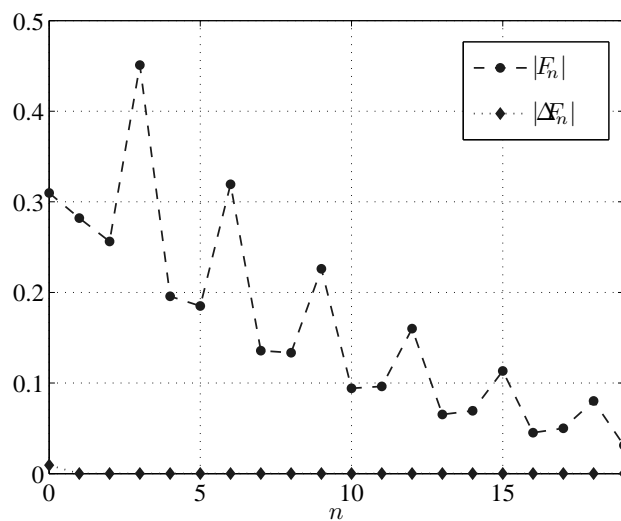


Figure 5.2: Magnitude of the expansion coefficients.



# Conclusions

In this work the analysis of the shielding effect of open and planar metallic (PEC) structures has been discussed; an analytic approach has been developed, achieving a closed form solution for the magnetostatic problem (representing a good approximation for ELF shielding) and an effective semi-analytic solution for the electromagnetic case. A key role in the entire work has been played by the representation unknown induced current, most of the presented results have been possible thanks to the factorizing of the diverging behaviour at the edges. All the results have been validated by a comparison with FEM simulations.

- In chapter 2 a magnetostatic analysis of a finite width thin PEC strip has been presented. The problem of the evaluation of the induced current on a thin strip in presence of a stationary line current, formulated in terms of a Cauchy's type integral equation, has been solved achieving a closed form expression for both the induced current and the magnetic field in the whole space. The magnetic shielding factor has been evaluated and some plots show its behaviour. Moreover, a comparative analysis between the proposed magnetostatic (ELF) solution and the one known in literature has been carried out, highlighting an interesting difference due to the critical choice of the current returning conductor.
- In chapter 3 a full-wave electromagnetic analysis for several thin PEC structure has been introduced. A semi-analytic solution of the integral problems, by means of an adequate expansion of the unknown in terms of orthogonal polynomials, has been achieved. This solution method provides an useful tool for the simulation of several shielding scenarios.

- In chapter 4 the analysis has been extended to thick PEC strip. The finite thickness of the metallic plate has been taken into account by the evaluation of the induced current on the four walls of a rectangular metallic structure and expanding these currents according to the Neumann series.
- In chapter 5 an improved method for the electromagnetic solution of thin structures has been developed. The method introduced in chapter 3 does "suffer" as the source line current is very close to the metallic shield. Hence, the magnetostatic solution has been proved to be an useful tool to improve and to accelerate the series convergence of the electromagnetic one.
- The appendix A does show how the expression of the electromagnetic field sustained by a single indefinite current line has been calculated.

The contributes of this work can be summarized as follows

- A new analytic magnetostatic solutions, which opens also a discussion about the conformal mapping solution validity in some cases.
- An accurate semi-analytic solution for several planar structure, which overcomes some of the limitation of FEM simulations and literature solutions .
- A new wave to approach the induced current on a PEC wedge and the consequent field scattering.
- An accelerating procedure based on a magnetostatic solution.

The achieved results can open interesting opportunity for future developments:

- Removing the hypothesis of PEC materials, facing the modelling issue of either real conductive and magnetic materials.
- Shields design tools and charts developed.
- Experimental validation

# Appendix A

## Line current source

In this appendix the expression of the electromagnetic field sustained by an line current  $I(\omega)$ , indefinite along the z-axis, is calculated. The geometry is depicted in Figure A.

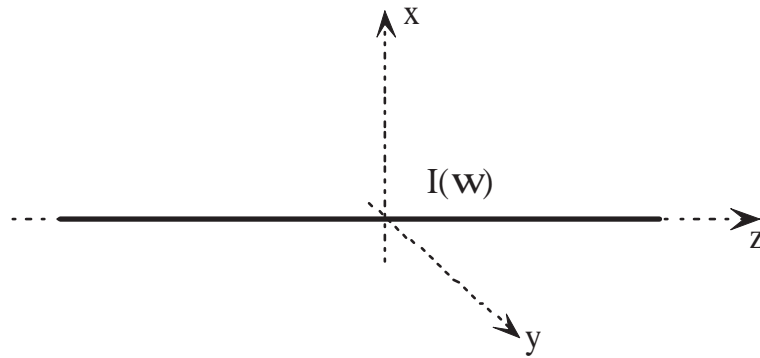


Figure A.1: Line current source

The impressed current density can be written as

$$\mathbf{J}(x_s, y_s, z_s) = I(\omega)\delta(x_s)\delta(y_s)\hat{z}, \quad (\text{A.0.1})$$

where  $(x_s, y_s, z_s)$  is a source point. The distance between a generic point  $(x, y, x)$  and a source point is

$$\sqrt{x^2 + y^2 + (z - z_s)^2} = \sqrt{r^2 + (z - z_s)^2} \quad (\text{A.0.2})$$

assuming  $r$  as the distance on the transverse  $(x, y)$  plane. Reminding the general expression for the vector potential

$$\mathbf{A}(P) = \frac{\mu}{4\pi} \int_S \mathbf{J}(P_s) \frac{e^{-jk|P-P_s|}}{|P - P_s|} dP_s \quad (\text{A.0.3})$$

where  $P$  and  $P_s$  are, respectively, the point in which the potential is evaluated and the source point,  $S$  signifies that the integration is extended to the whole source region and  $k = \omega\sqrt{\varepsilon_0\mu_0}$  is the wave-number.

In this case the vector potential becomes

$$A_z(r) = \frac{\mu}{4\pi} I(\omega) \int_{-\infty}^{\infty} \frac{e^{-jk\sqrt{r^2+(z-z_s)^2}}}{\sqrt{r^2+(z-z_s)^2}} dz_s = \frac{\mu}{4\pi} I(\omega) \int_{-\infty}^{\infty} \frac{e^{-jk\sqrt{r^2+u^2}}}{\sqrt{r^2+u^2}} du, \quad (\text{A.0.4})$$

it is clear that, in force of the symmetry,  $\mathbf{A}$  is not depending on  $z$ .

Thanks to the integral representation of the Hankel function of second kind  $H_0^{(2)}$  [31]

$$\int_{-\infty}^{\infty} \frac{e^{-jk\sqrt{r^2+u^2}}}{\sqrt{r^2+u^2}} du = \frac{\pi}{j} H_0^{(2)}(kr), \quad (\text{A.0.5})$$

the vector potential can be rewritten as

$$A_z(r) = \frac{\mu}{4j} I(\omega) H_0^{(2)}(kr). \quad (\text{A.0.6})$$

The well known relations for the fields  $\mathbf{E}$  and  $\mathbf{H}$  in terms of vector potential

$$\mathbf{E} = -j\omega\mathbf{A} + \frac{\nabla\nabla \cdot \mathbf{A}}{j\omega\varepsilon_0\mu_0} \quad (\text{A.0.7})$$

$$\mathbf{H} = -\frac{1}{\mu_0} \nabla \times \mathbf{A} \quad (\text{A.0.8})$$

where, in this case

$$\nabla \nabla \cdot \mathbf{A} = 0, \quad (\text{A.0.9})$$

lead to the following

$$E_{0z}(r) = -j\omega A_z \quad (\text{A.0.10})$$

$$H_{0\varphi}(r) = -\frac{1}{\mu_0} \frac{dA_z}{dr}. \quad (\text{A.0.11})$$

Thus, by the adequate substitutions,

$$E_{0z}(r) = -\frac{\omega\mu}{4} I(\omega) H_0^{(2)}(kr), \quad (\text{A.0.12})$$

$$H_{0\varphi}(r) = \frac{k}{4j} I(\omega) H_1^{(2)}(kr). \quad (\text{A.0.13})$$

It is worth noting that in the magnetostatic case, namely  $\omega = 0$

$$E_{0z}(r) = 0, \quad (\text{A.0.14})$$

$$H_{0\varphi}(r) = \frac{I}{r} \delta(\omega). \quad (\text{A.0.15})$$

In force of the above considerations, the electromagnetic field generated by a line current, indefinite along the z-axis and displaced at  $x = a$  and  $y = b$ , is

$$\mathbf{E}_0(x, y) = -\hat{z} \zeta_0 \frac{k}{4} I(\omega) H_0^{(2)} [k\sqrt{(x-a)^2 + (y-b)^2}], \quad (\text{A.0.16})$$

$$\mathbf{H}_0(x, y) = \hat{\varphi} \frac{k}{4j} I(\omega) H_1^{(2)} [k\sqrt{(x-a)^2 + (y-b)^2}], \quad (\text{A.0.17})$$

where  $\zeta_0 = \sqrt{\mu_0/\varepsilon_0}$  is the characteristic impedance of the free space.

Thus, in cartesian coordinates, the fields can be written as

$$E_{0z}(x, y) = -\zeta_0 \frac{k}{4} I(\omega) H_0^{(2)} [k\sqrt{(x-a)^2 + (y-b)^2}], \quad (\text{A.0.18})$$

$$H_{0x}(x, y) = \frac{k}{4j} \frac{I(\omega)(y-b)}{\sqrt{(x-a)^2 + (y-b)^2}} H_1^{(2)} [k\sqrt{(x-a)^2 + (y-b)^2}], \quad (\text{A.0.19})$$

$$H_{0y}(x, y) = \frac{k}{4j} \frac{I(\omega)(a-x)}{\sqrt{(x-a)^2 + (y-b)^2}} H_1^{(2)} [k\sqrt{(x-a)^2 + (y-b)^2}]. \quad (\text{A.0.20})$$



# Bibliography

- [1] S. Levy, *Electromagnetic shielding effect of an infinite plane conducting sheet placed between circular coaxial coils*, Proc. IRE, vol.21,pp. 923-941,June 1936.
- [2] Schelkunoff SA, *Electromagnetic waves*, Van Nostrand, Princeton 1943.
- [3] K.F. Casey, *Low-frequency penetration of loaded apertures*, IEEE Trans. on Electromagnetic Compatibility, vol. EMC-23, pp.367-377, Nov. 1981.
- [4] L. Hasselgren and J. Luomi, *Geometrical aspects of magnetic shielding at extremely low frequencies*, IEEE Trans. on Electromagnetic Compatibility, vol. 37, pp. 409-420, Aug. 1995.
- [5] J. F. Hoburg, *Principles of quasi-static magnetic shielding with cylindrical and spherical shields*, IEEE Trans. on Electromagnetic Compatibility, vol. 37, pp. 574-579, Nov. 1995.
- [6] C. M. Ryan, *A computer expression for predicting shielding effectiveness for the low-frequency plane-shield case*, IEEE Trans. on Electromagnetic Compatibility, vol. EMC-9, pp. 83-94, Mar. 1967.
- [7] J.R. Moser, *Low-frequency shielding of a circular loop electromagnetic field source*, IEEE Trans. on Electromagnetic Compatibility, vol. EMC-9, pp. 6-18, Mar. 1967.
- [8] P.R. Bannister, *New theoretical expressions for predicting shielding effectiveness for the plane shield case*, IEEE Trans. on Electromagnetic Compatibility, vol. EMC-10, pp. 1-7, Mar. 1968.

- 
- [9] P.R. Bannister, *Further notes for predicting shielding effectiveness for the plane shield case*, IEEE Trans. on Electromagnetic Compatibility, vol. EMC-11. pp. 50-53, May 1969.
- [10] J.R. Moser, *Low frequency low-impedance electromagnetic shielding*, IEEE Trans. on Electromagnetic Compatibility, vol. 30, pp. 202-210, Aug. 1988.
- [11] Schulz RB, Plantz VC, Brush DR, *Shielding theory and practice*, IEEE Trans. on Electromagnetic Compatibility 30(3):187201 (1988)
- [12] K. F. Casey, *Electromagnetic shielding behavior of wire-mesh screens*, IEEE Trans. on Electromagnetic Compatibility, vol. 30, pp. 298-306, Aug. 1988.
- [13] J. R. Wait, *Electromagnetic shielding of sources within a metal-cased bore hole*, IEEE Trans. on Geoscience Electronics, vol. GE-15, pp. 108-112, Apr. 1977.
- [14] J.F. Hoburg, *Principles of quasi-static magnetic shielding with cylindrical and spherical shields*, IEEE Trans. on Electromagnetic Compatibility, vol. 37, pp. 574-579, NOV. 1995.
- [15] J.F. Hoburg, *A computational methodology and results for quasi-static magnetic shielding*, IEEE Trans. on Electromagnetic Compatibility, vol. 38, pp. 92-103, Feb. 1996.
- [16] E. H. Newman and M. Kragalott, *Moment method analysis of the electric shielding factor of a conducting TM shield at ELF*, IEEE Trans. on Electromagnetic Compatibility, vol. 37, pp. 400-408, Aug. 1995.
- [17] T. Rikitake, *Magnetic and Electromagnetic Shielding*. Boston, MA: D. Reidel, 1987.
- [18] Z Yichao et al., *Analysis and Test of EM Shielding for Low-Frequency Magnetic Field*, EMC 2007. International Symposium on Electromagnetic Compatibility, 2007

- [19] C. Buccella et al., *Magnetic Field Computation in a Physically Large Domain With Thin Metallic Shields*, IEEE Trans. On Electromagnetic Compatibility, Vol. 41, No. 5, May 2005
- [20] R. Estrada, Ram. P. Kanwal, *Singular Integral Equations* (Birkhäuser, Boston 2000) pp. 71-123, 324
- [21] S. Celozzi, G. Panariello, F. Schettino, L. Verolino, *Analysis of the induced currents in finite size PCB ground plane*, Electrical Engineering, **Vol. 83**, (2001)
- [22] Robert G. Olsen, P. Moreno *Some Observations About Shielding Extremely Low-Frequency Magnetic Fields by Finite Width Shields*, IEEE Trans. on Electromag. Compat. vol. EMC-38 (Aug, 1996) pp. 460-468.
- [23] J. J. Meixner, *The behavior of electromagnetics fields at the edges*, IEEE Trans. on Antennas and Propagation vol. AP-20, no. 4, (1972) pp. 442-446.
- [24] F. Oberhettinger, L. Badii, *Tables of Laplace Transforms*, Springer Verlag, Berlin 1973
- [25] R. G. Olsen, M. Istenič, *Simple hybrid method for ELF shielding by imperfect finite planar shields*, IEEE Trans. on Electromag. Compat. vol. EMC-46 (May, 2004) pp. 199-207.
- [26] K. J. Binns and P. J. Lawrenson, *Analysis and Computation of Electric and Magnetic Field Problems*, New York: Pergamon, 1973.
- [27] V. Comincioli, *Analisi numerica*, McGraw-Hill Italia, Milano, 1995.
- [28] IEEE 229, *IEEE Standard method for measuring the effectiveness of electromagnetic shielding of enclosures*, (1991)
- [29] K. Eswaran, *On the solution of a class of dual Integral Equations Occuring in Diffraction Problems*, Proc. Royal Society, London, 1990.

- [30] M. Abramovitz, I. Stegun, *Handbook of mathematical function*, 9th Edition, Dover, New York, 1972.
- [31] I. S. Gradshteyn, I. M. Ryzhik, *Table of Integrals, Series and Products*, (Academic press, New York 1980)